Received: 16 March 2018 | Revised: 7 June 2018 | Accepted: 19 June 2018
DOI: 10.1002/jemt.23094

WILEY MICROSCOPY RESEARCH & TECHNIQUE

REVIEW ARTICLE

Fundus image classification methods for the detection of glaucoma: A review

Tanzila Saba[1] | Syedia Tahseen Fatima Bokhari[2] | Muhammad Sharif[2] | Mussarat Yasmin[2] | Mudassar Raza[2]

[1]College of Computer and Information Sciences, Prince Sultan University, Riyadh, Saudi Arabia

[2]Department of Computer Science, COMSATS University Islamabad, Wah Campus, Pakistan

Correspondence
Tanzila Saba, College of Computer and Information Sciences, Prince Sultan University, Riyadh 11586, Saudi Arabia.
Email: drstanzila@gmail.com

Review Editor: Prof. Alberto Diaspro

Abstract

Glaucoma is a neurodegenerative illness and is considered as a standout amongst the most widely recognized reasons for visual impairment. Nerve's degeneration is an irretrievable procedure, so the diagnosis of the illness at an early stage is an absolute requirement to stay away from lasting loss of vision. Glaucoma effected mainly because of increased intraocular pressure, if it is not distinguished and looked early, it can result in visual impairment. There are not generally evident side effects of glaucoma; thus, patients attempt to get treatment just when the seriousness of malady is advanced altogether. Determination of glaucoma often comprises of review of the basic crumbling of the nerve in conjunction with the examination of visual function capacity. This article shows the persistent illustration of glaucoma, its side effects, and the potential people inclined to this malady. The essence of this article is on different classification methods being utilized and proposed by various scientists for the identification of glaucoma. This article audits a few division and segmentation methodologies that are exceptionally useful for recognizable proof, identification, and diagnosis of glaucoma. The research related to the findings and the treatment is likewise evaluated in this article.

KEYWORDS

cup to disc ratio, intraocular pressure, open angle glaucoma, progression detection, risk analysis

1 | INTRODUCTION

Glaucoma is an eye disorder that within the eyes yields intraocular pressure (IOP) (Masood, Sharif, Masood, Yasmin, & Raza, 2015; Masood, Sharif, Raza, et al., 2015; Sommer et al., 1991). The IOP increases by the damage of the optic nerves as the time progresses (Köse & Ikibaşs, 2011; Nayak, Acharya, Bhat, Shetty, & Lim, 2009; Noronha, Acharya, Nayak, Martis, & Bhandary, 2014; Toshev, Lamparter, Pfeiffer, & Hoffmann, 2017). Medicine can be used to avoid vision loss, as there is no treatment for glaucoma. Usually, through the trabecular meshwork aqueous humor streams out of the eye, but when this passage is blocked, this fluid rises in the eye (Acharya et al., 2015; Chrástek et al., 2005). Glaucoma amongst retinal diseases is the most common and prominent reason for vision loss that ultimately leads to blindness (Roodhooft, 2002). Changes are caused by retinal structures because of the presence of glaucoma, which causes progressive vision loss if not treated in time and eventually leads to permanent blindness. There does not exist any proper way till now to treat glaucoma but if we want to prevent blindness, early identification of glaucoma can play a vital role. As the manual investigative process is expensive and may lead to errors, some automatic glaucoma detection exertions have been made at an early stage. A comprehensive review of retinal images related to existing methods is very important for glaucoma-related automatic identification and detection of structural features. Amongst a group of eye disorders, glaucoma is the one that is related to the visual field's functional failure. The functional changes are revealed by a gradually shrinking neuro-retinal rim representing in the optic nerve, a deterioration of astrocytes and axons (Michelson, Wärntges, Hornegger, & Lausen, 2008). The organization of the remaining sections are delineated as takes after: glaucoma is portrayed briefly in Section 2 along with glaucoma-related changes in retinal structures. Section 3 portrays, the scientific and clinical techniques used currently for Glaucoma analysis and diagnosis. Section 4 provides an overview of automatic retinal features detection associated with Glaucoma using the existing classification and segmentation (Irum, Raza, & Sharif, 2012; Masood, Sharif, Masood, et al., 2015; Masood, Sharif, Raza, et al., 2015) methods in a systematic way. Section 5 presents the conclusion. The list of abbreviations is shown in Table 1.

1.1 | What is actually glaucoma?

Glaucoma is caused by the increased IOP in eyes and hence considered as among one of the reasons for vision misfortune that in the long run prompts visual impairment (Bokhari, Sharif, Yasmin, & Fernandes, 2017). Gaucoma occurs because of increased IOP, optic nerve fibers (ONF), and axons decrease. ONF decreases the thickness of retinal fiber layer (RNFL) while axons cause changes in ONH configuration, expands cup size, and decreases neuro-retinal thickness hence, retinal functional capability decreases (Bock, Jörg, Georg, László, & Joachim, 2007; Shabbir, Sharif, Nisar, Yasmin, & Fernandes, 2016). Ophthalmologists can, without much of a stretch, identify these progressions by utilizing Ophthalmoscopy orstereo fundus photography of ONH (Betz, Camps, Collignon-Brach, Lavergne, & Weekers, 1982).

1.2 | Types of glaucoma

Glaucoma exists in numerous types; angle-closure glaucoma (ACG) and primary open-angle glaucoma (POAG) are the two utmost communal categories of glaucoma (See Table 2 for detail) (Giaconi, Law, & Nouri-Mahdavi, 2016). Other forms of glaucoma are pigmentary glaucoma, acute glaucoma, normal pressure glaucoma, angle recession glaucoma, cognital glaucoma, exfoliative glaucoma, steroid induced glaucoma, chronic glaucoma, secondary glaucoma, and neovascular glaucoma (see Figure 1 for hierarchy).

1.3 | Individuals at risk for glaucoma?

Figure 2 depicts some risk factors for Glaucoma. It does not mean that if an individual's eye pressure has increased then that person is suffering from glaucoma, but it is considered as an important risk factor (Kourkoutas et al., 2012). The risk of the disease development will be determined by an ophthalmologist. Amongst some of the most important risk factors comprise - higher eye pressure (NY, 2009), persons belonging from (Africa, America, or Latino), thin cornea, age, individuals suffering from hypertension and diabetes (may considered to have higher risk factor of developing OAG), family history of glaucoma, having cardiovascular disease, nearsightedness, past injuries to the eyes, steroid use, blood pressure rate, persons having myopia, and a history of severe anemia. The researchers found that 17% people with hypertension, 35% persons with diabetes and 48% people having both hypertension and diabetes were more prone to developing OAG. A collection of conditions that are associated with metabolic syndrome's components includes hypertension, hyperlipidemia (high cholesterol and triglyceride levels), obesity, and diabetes. The researchers establish that persons having hypertension and diabetes increased the risk of OAG. More research is underway to develop treatments that could be used for treating glaucoma and assess whether it is the hyperlipidemia, or not that decrease the risk of glaucoma.

For specific treatment, each factor signifies a potential target that is why risk factor concept is considered to be very important (Staal, Abràmoff, Niemeijer, Viergever, & van Ginneken, 2005). For the transformation to glaucoma regarding risk factors for ocular hypertension, some large, longitudinal, and prospective studies have provided evidence. To provide authentication of a prediction model for the glaucoma development the ocular hypertension treatment study (OHTS) (Bubella, Bubella, & Cillino, 2014), and European glaucoma prevention study (GPS) (Gordon et al., 2002) are the two clinically randomized judgments being used. For the potential association between risk conversion to glaucoma through both the studies, many predictive factors have been evaluated. Digital color fundus images are a widespread imaging modality to predict glaucoma nowadays (Akbar, Akram, Sharif,

TABLE 1 Abbreviations

Symbol	Description	Symbol	Description
RNFL	Retinal nerve fiber layer	SLP	Scanning laser polarimetry
ONF	Optic nerve fibers	FDT	Frequency doubling technology Perimetry
POAG	Primary open-angle glaucoma	CAD	Computer-aided diagnosis
ACG	Angle-closure glaucoma	HRT	Heidelberg retina tomography
CDR	Cup to disc ratio	HOS	Higher order spectra
IOP	Intra ocular pressure	STARE	Structured analysis of retina
OHTS	Ocular hypertension treatment study	ANN	Artificial neural networks
EGPS	European glaucoma prevention study	PCA	Principle component analysis
RNFL	Retinal fiber layer	KNN	k-nearest neighbor
mfERG	Multifocal electroretinography	SVM	Support vector machine
CSLT	Confocal scanning laser tomography	ROC	Receiver operating curve
SDOCT	Spectral-domain optical coherence tomography	DWT	Discrete wavelet transform
EG	Experimental Glaucomas	FCM	Fuzzy C-means clustering
VCD	Vertical cup diameter	RACAL	Radius-based clustering algorithm
VDD	Vertical disc diameter	LDA	Linear discriminate analysis
VFT	Visual field testing	GPS	Glaucoma probability score
SLP	Scanning laser Perimetry	MD	Multidimensional distances
ONE	Optic nerve evaluation	ISNT	Inferior superior nasal temporal
SWAP	Short wavelength automated Perimetry	CNN	Convolution neural network
CSLO	Confocal scanning laser ophthalmoscopy	GVF	Gradient vector flow
SAP	Standard automated Perimetry	ASM	Active shape models
NB	Naïve Bayesian	ACM	Active contour model
RT	Radon transform	SLIC	Simple linear iterative clustering

TABLE 2 Types, causes, and symptoms of glaucoma

Types of glaucoma	Progression	Causes	Symptoms
Open-angle glaucoma	Amongst the most communal type of glaucoma is OAG. As it is pain-free (individual does not feel any pain) and its rate of advancement is slow so, patients may only notice vision loss when the disorder progressed significantly (Dua, Acharya, Chowriappa, & Sree, 2012).	As it has no symptoms till substantial vision loss has arisen so this form of glaucoma is commonly termed "the sneak thief of sight" (Friedman et al. 2004).	Typically considered, there are no early indications of OAG. For many years, keeps on progressing slowly and at times without visible vision loss. Typically, in both the eyes, damage to peripheral vision gets damaged steadily which leads to prompts limited focus in the propelled stages.
Angle-closure glaucoma	The ACG is agonizing (painful) and abrupt that is the reason there is a loss of vision at a noteworthy rate (Manners, Salmon, Barron, Willies, & Murray, 2001).	Angle-closure is a much more exceptional form of glaucoma that requires immediate medical treatment as it progresses very rapidly.	Symptoms of ACG are vomiting/ regurgitating (related with serious eye torment), extreme eye and head torment, obscured or indistinct vision, the presence of rainbow-hued hovers around splendid lights, quick sight misfortune.
Low-tension glaucoma	It is not necessary that all forms of glaucoma are categorized by intra-ocular pressures. Even eye pressures are normally maintained, but damage occurs in the optic nerve, bringing about visual field misfortune in case of normal-tension or low-tension glaucoma.	This type of glaucoma occurs because of poor blood development. This type occurs generally in Japanese or in people who have a background marked by the vascular disease (Nayak et al., 2009).	Because of the increase in the IOP as compared to other eyes, eyes suffering from this disorder are far more susceptible to damaging optic nerves. The exclusive focus is the manifestation that can distinguish low tension glaucoma however until that point, a perpetual harm to optic nerve would have occurred.
Exfoliation syndrome (exfoliative glaucoma)	A common form of OAG is exfoliation syndrome.	Laser treatment generates better results for this form of glaucoma. This sort of glaucoma is, for the most part, analyzed in the European of northern descent (Noronha et al., 2014).	In exfoliation syndrome, abnormal generation of whitish material appears on the lens and retinal drainage angle of the eye. This whitish material along with fluid present at the back of iris can block the eye drainage system, resulting in increased IOP.
Pigmentary glaucoma	Pigmentary glaucoma typically affects young, near-sighted, white males. In this condition, the iris comes into interaction with support structures, bows backward for holding the lens in place.	The cells that are facing the iris get interrupted through this situation containing pigment at the back surface so, pigment particles are released into the drainage system causing increased IOP of the eye that eventually block the drainage system. The blockage in drainage angle may damage the drainage system too (Rajendra Acharya et al., 2015).	Glaucoma of this sort, for the most part, does not demonstrate any side effects. The main indication detectable can be a little agony in the eye and hazy vision after exercise. Laser treatment generates better results for this form of glaucoma.
Steroid-induced glaucoma	Sometimes the IOP exceeds in the eye causing damage to optic nerves it starts to develop glaucoma or eventually causes vision loss.	Damaging optic nerves because of increased IOP.	Glaucoma brought about by this sort is essentially incited by the high rise in the eye through intraocular push/ stress (Chrástek et al., 2005).
Neovascular glaucoma	The drainage system of the eye gets affected by numerous diseases, including diabetes that causes the blood vessels to rise on the iris.	The fluid's drainage system gets properly blocked (Roodhooft, 2002).	–
Angle recession glaucoma		This kind of glaucoma happens when the injured tissue from some first enduring hampers the consumption of the fluid.	This sort of glaucoma may traverse after the novel injury or might develop years (Michelson et al., 2008).
Congenital glaucoma	Congenital glaucoma is ordinarily present in somebody from his/her birth (introduction to the world) and is a type of acquired glaucoma (Bock et al., 2007).	This sort can be analyzed and diagnosed with ones age. These patients, for the most part, have an issue with their seepage/ drainage framework or have a narrow-angle.	The issue with such sort of glaucoma is that it happens at early ages and patients around then cannot comprehend the issues going ahead with them. It predominantly happens in boys (Betz et al., 1982).
Secondary glaucoma	Secondary glaucoma is a kind of glaucoma when the intraocular pressure within the eye is expanded by some other eye issue.	Other restorative difficulties most often result in this sort of glaucoma (Giaconi et al., 2016). Both OAG and ACG can be primary or auxiliary conditions.	This sort of glaucoma more often happens in situations like surgery, inflammation etc. (Dua et al., 2012).

(*Continues*)

TABLE 2 (Continued)

Types of glaucoma	Progression	Causes	Symptoms
		Secondary/auxiliary conditions are called primary when the cause is obscure then it is considered yet if the condition can be followed to a known cause to bring about, for example, irritation, medicines, eye damage then the condition is called auxiliary/secondary.	
Acute glaucoma	This kind of glaucoma happens when the development of the liquid inside the eye is totally obstructed from drainage. With a specific end goal to make it conceivable, the narrow-angle closes itself (Friedman et al., 2004).	This sort can bring about enduring devastation if not considered in time. Sometimes, it becomes exceptionally difficult and aching however now and again, it does not bring about sudden pain (Ng et al., 2015).	The side effects of this kind of glaucoma incorporate red eyes, queasiness, vomiting, and faintness.
Chronic glaucoma	In this form of glaucoma, there is progressively decrease in vision	For the cure of this disease and keeping the damage to the limited stage, early handling is necessary (Greenfield et al., 2007).	The major issue in this form of glaucoma is that once the damage occurs in vision, it cannot be repaired.

Tariq, & Yasin, 2017; Bokhari, Syedia, Sharif, Yasmin, & Fernandes, 2018; Khan, Sharif, Yasmin, & Fernandes, 2016; Khan, Sharif, Yasmin, & Saba, 2017; Qureshi, Sharif, Yasmin, Raza, & Javed, 2016). For measuring the optic nerve damage from fundus images, various features can be extracted. The factors considered to detect glaucoma include neuro-retinal rim notching, peripapillary atrophy, RNFL, neuroretinal rim thinning, the optic cup-to-disc ratio (CDR), disc haemorrhage and inter-eye asymmetry defect. The persons suffering from hyperlipidemia, the chances of glaucoma and diabetic retinopathy are enhanced (Akbar, Akram, Sharif, Tariq, & Yasin, 2018; Amin, Sharif, Yasmin, Ali, & Fernandes, 2017; Amin et al., 2016; Station, 2007).

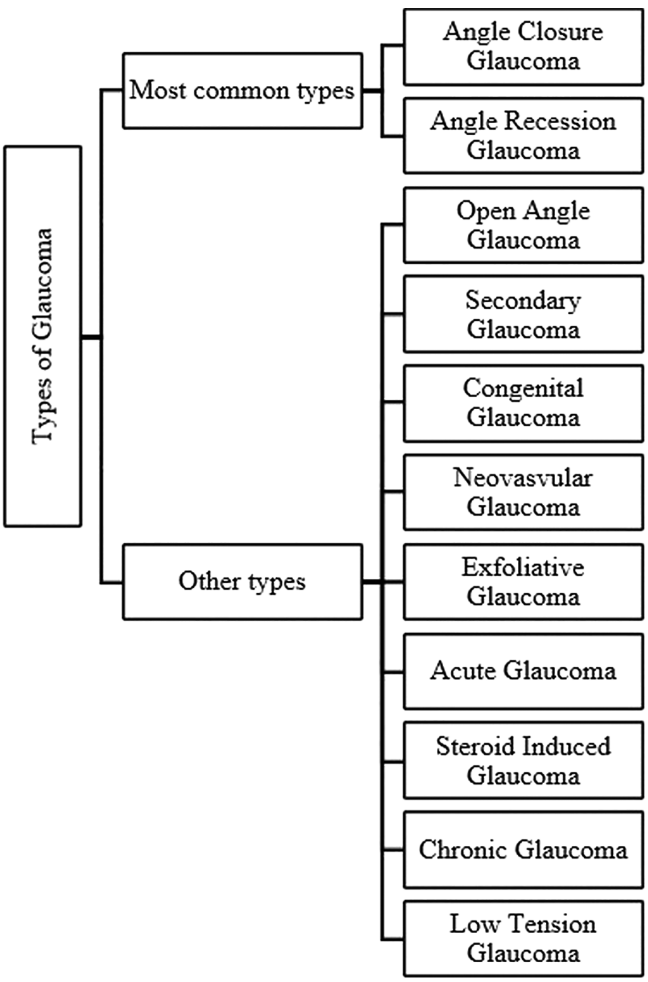

FIGURE 1 Frequent categories of glaucoma (Khaimi, 2015; Masood, Sharif, Masood, Yasmin, & Raza, 2015; Masood, Sharif, Raza, et al., 2015)

2 | PROGRESSION DETECTION MEASURE

For diagnosing glaucoma (Jonas et al., 2017) and measuring how much glaucoma has progressed in eyes, Geometric parameters of the ONH (Newman-Casey, Talwar, Nan, Musch, & Stein, 2011). Geometric constraints are employed in (Miglior et al., 2003) that RF classifier gives

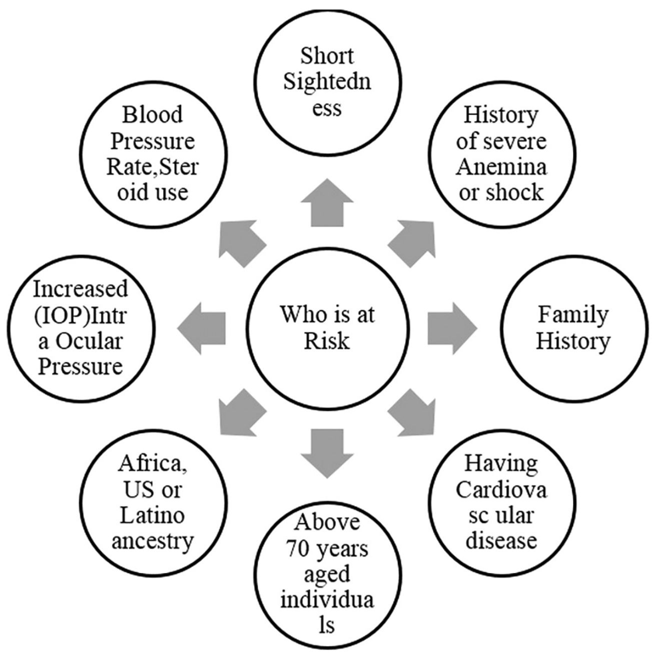

FIGURE 2 Risk factors for glaucoma (Kim et al., 2014; Zafar et al., 2018)

TABLE 3 CDR size in different glaucomatous stages

Stages of glaucoma	Cup to disc ratio (CDR)	Effects on eyes
Mild glaucoma	0.4	Very less visual loss occurs in the mild stage of glaucoma (side or peripheral).
Moderate glaucoma	0.5–0.7	Central vision may remain unaffected in moderate glaucoma.
Severe glaucoma	Above 0.7	The extreme loss of ONF happens, optic nerve hemorrhages, and the presence of central indents, that is, foveal notches (He et al., 2013) in severe glaucoma stage. If remained uncontrolled then the patient may lose vision.

better forecast exactness contrasted with other machine learning systems including outspread premise work, multilayer perceptron, Bayes net and naive Bayesian tree classifiers. The detection of multifocal electroretinography (mfERG), ONH, for leading towards the exposure of ONH surface, CSLT is used (Abdel-Ghafar & Morris, 2007).

2.1 | CDR value in healthy and persons suffering from different stages of glaucoma

CDR in a normal individual is usually 0.3. The seriousness of glaucoma increments with the expansion in CDR. To compute CDR, the clinical convention is followed. To measure CDR, the ratio between the Vertical Cup Diameter (VCD) and Vertical Disc Diameter (VDD) is used.

$$\mathrm{CDR} = \frac{\mathrm{VCD}}{\mathrm{VDD}}$$

For the transmission of glaucoma, CDR is calculated. If the threshold value of CDR is larger than 0.3, then that eye is considered to be glaucomatous. However, if the threshold the limit esteem is not exactly or equivalent to threshold then the eye is thought to be ordinary or healthy. Table 3 depicts CDR size in different Glaucomatous Stages.

3 | GLAUCOMA DETECTION METHODS

For measuring the early damage caused by glaucoma, a combination of test types without a significant drop in specificity may be beneficial (Konstas et al., 2007; Li, Lim, Liu, Mitchell, et al., 2010).

To observe the effect of glaucoma at regular intervals, visual field testing (VFT) and Optic nerve evaluation (ONE) are accomplished. It is done to indicate the effectiveness of the treatment being used by these tests to observe whether further treatment is required or not. These tests are not essential at every visit for every person. The fundamental research target of the examination is to discover if glaucoma damage has progressed with the passage of time. Figure 3 shows different tests used in Glaucoma Detection.

3.1 | Glaucoma diagnostic approaches

The detection methods start with noise removal (Irum, Shahid, Sharif, & Raza, 2015; Irum, Sharif, Raza, & Mohsin, 2015; Irum, Sharif, Raza, & Yasmin, 2015; Irum, Sharif, Yasmin, Raza, & Azam, 2015), upgrade/enhancement taken after by feature extraction, feature optimization and afterwards at last recognizable proof of the presence of glaucoma. Other diagnostic approaches are segmentation, morphology, image fusion, image registration, classification, pattern matching, and statistical measurement etc. (Cheng, Yin, Wong, Tao, & Liu, 2015). For glaucoma detection method mfERG and Optical coherence tomography (OCT) (Li, Lim, Liu, Wing, et al., 2010) techniques are used. Both OCT and (mfERG) are used to compute the progression detection of glaucoma, examining functional and structural and to observe inconsistency in the eyes accurately. In recent years, CAD is assuming a noteworthy part of screening glaucoma (Miguel-Jiménez, Boquete, Ortega, Rodríguez-Ascariz, & Blanco, 2010). The decision system for glaucoma can separate ordinary and glaucoma cases precisely (He et al., 2013). For the evaluation of SLP, OCT, and HRT, methods can be used by utilizing retinal ONF layer. In a range of diseases for the monitoring and diagnosis of retinal damage, OCT has as of late turned into an effective tool in medicine (Nath & Dandapat, 2012). It gives organic tissues having cross-sectional images of high determination utilizing non-obtrusive imaging innovation (Acharya, Dua, Du, Sree, & Chua, 2011). Spectral Domain OCT gives better results as compared to Confocal Scanning Laser Ophthalmoscopy (Toshev et al., 2017). A multimethodology fusion based glaucoma distinguishing proof and treatment approach is presented and talked about in (Acharya et al., 2011) by taking part patient's information, chief ocular image highlighted features and significant genome SNPs structures in one framework.

3.2 | Treatment for glaucoma

The treatment for glaucoma involves medical management eye drops (Sung et al., 2011), trabeculectomy or microsurgery (Wang, Khan, & Coleman, 2015), laser surgery (Mermoud et al., 1999; Zafar, Sharif, & Yasmin, 2018) and drainage implants. Figure 4 depicts the different types of glaucoma treatments.

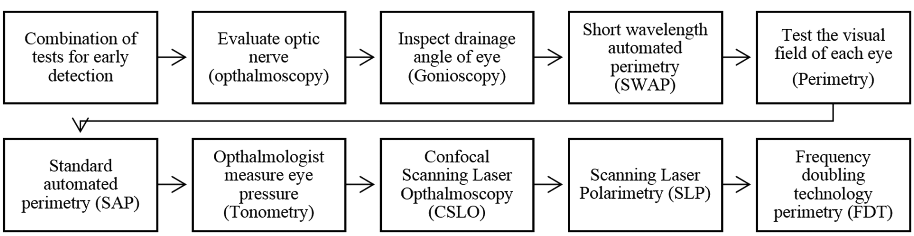

FIGURE 3 Different tests used in glaucoma detection (Choplin & Traverso, 2014)

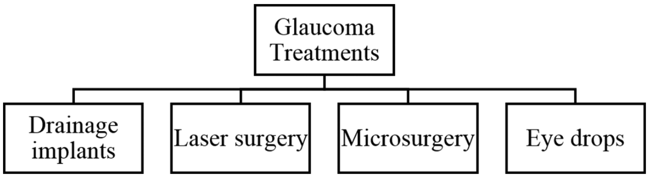

FIGURE 4 Types of glaucoma treatments (Masood, Sharif, Masood, Yasmin, & Raza, 2015; Masood, Sharif, Raza, et al., 2015; Rosenfeld, Price, Lai, Witzmann, & Price, 2015)

4 | PUBLIC DATASETS USED FOR CLASSIFICATION

From the literature review, brief explanations of the public databases are explained in this section. Datasets are constructed most of which are available publically for the anatomical structures utilized for glaucoma finding like the optic papilla (disk) yet programmed include extraction is done in the greater part of the datasets for Diabetic Retinopathy. For extracting the features automatically particularly for Glaucoma, some of the publically available datasets were constructed. In the literature, various researchers performed identification, detection, risk prediction, and progression detection of glaucoma using different datasets (Table 4). Comprising of varying number of images each data set to hold out images some comprise of normal eye images and other are retinal glaucomatous images representing images in different stages of glaucoma.

TABLE 4 Public datasets used for classification

Reference	Dataset	Images
Acharya et al. (2009)	ACHIKO-O or ORIGA light	650 retinal images amongst them 168 images are glaucomatous, while 482 are non-glaucomatous
Zhang et al. (2010)	ACHIKO-K	258 images with segmentation annotations
Zhang et al. (2013)	ACHIKO-I	179 images separated into various subsets
Yin et al. (2013)	STARE	81 number of images. Out of the 81 images, the symptoms of the retinal disease are shown in 50 images that obscure optic nerve head completely, such as exudates and haemorrhages, and 31 are from fit retinas.
Hoover (2000)	RIM-ONE	169 images: 118 normal, 12 suffering from early glaucoma stage, 14 having moderate glaucoma symptoms, 14 having severe glaucoma and 11 suffering from ocular hypertension
Staal et al. (2004)	DRIVE	40 fundus images of 584 × 565 pixels resolution.
Balasubramanian et al. (2010)	DRION-DB	110 retinal images having 600 × 400 pixels resolution
Kauppi et al. (2007)	DIARETDB0	130 images at 1500 × 1152 pixels
Kauppi et al. (2007)	DIARETDB1	84 fundus images of size 1500 × 1152 pixels
Sng et al. (2012)	SCES	1676 images

5 | PATTERN CLASSIFICATION AND MACHINE LEARNING METHODS FOR GLAUCOMA DETECTION

Many image enhancement methods are used for the detection of glaucoma. Researchers have used different methodologies in their proposed work. Different types of databases have been collected comprising of varying number of images. By applying these images enhancement techniques using different classifiers, sensitivity, specificity, and accuracy of those techniques have been calculated. Figure 5 shows some classification methods used in Glaucoma identification and detection.

5.1 | Supervised methods

For learning feature extraction using retinal images, supervised methods are used. The performance of supervised methods is normally better as compared to unsupervised methods. As supervised strategies depend on pre-arranged information, and for healthy retinal images can produce extremely good results. For the division of retinal images, ANN systems have been widely inspected (Fraz et al., 2012) for choosing the probability of input data, these neural networks retain mathematical weights fitting into a particular output (Yasmin, Sharif, & Mohsin, 2013). SVM is a nondirect/linear classifier built upon the factual learning hypothesis that can arrange the new information accurately (Heryadi, Fanany, & Arymurthy, 2013). SVM is used for distinguishing healthy eyes from glaucomatous eyes and creates a hyperplane and utilizes multidimensional parameters into a feature space by considering the most extended distance among all cases and the hyperplane (Abdi & Williams, 2010). A novel automated glaucoma diagnosis method is counselled employing assorted features removed from Gabor change requested on digital fundus images. These expelled elements are subjected to PCA (Anantrasirichai, Achim, Morgan, Erchova, & Nicholson, 2013) expurgate the dimensionality of the components. Next, these components/features are positioned, utilizing arranged positioning strategies in particular: Bhattacharyya (Acharya et al., 2015) space calculation, *t*-test, Wilcoxon examination, ROC, and entropy. T-test positioning strategy yielded the most elevated introduction close by a normal precision of 93.10%, specificity of 96.20% and affectability of 89.75% utilizing 23 features include nearby SVM classifier (Bauer, Pereverzev, & Rosasco, 2007). For the diagnosis of glaucoma, various scanning methods can be utilized by utilizing OCT, SLP, and HRT through which the retinal ONF layer can be surveyed. As these methods are very expensive and hence for the diagnosis of glaucoma automatically, a novel low-priced course of action utilizing computerized fundus images is proposed (Mookiah, Rajendra Acharya, Lim, Petznick, & Suri, 2012). Naser Langroudi and Sadjedi (2010) worked on vessel identification by using multiscale Gabor filters then removed features employing main constituent

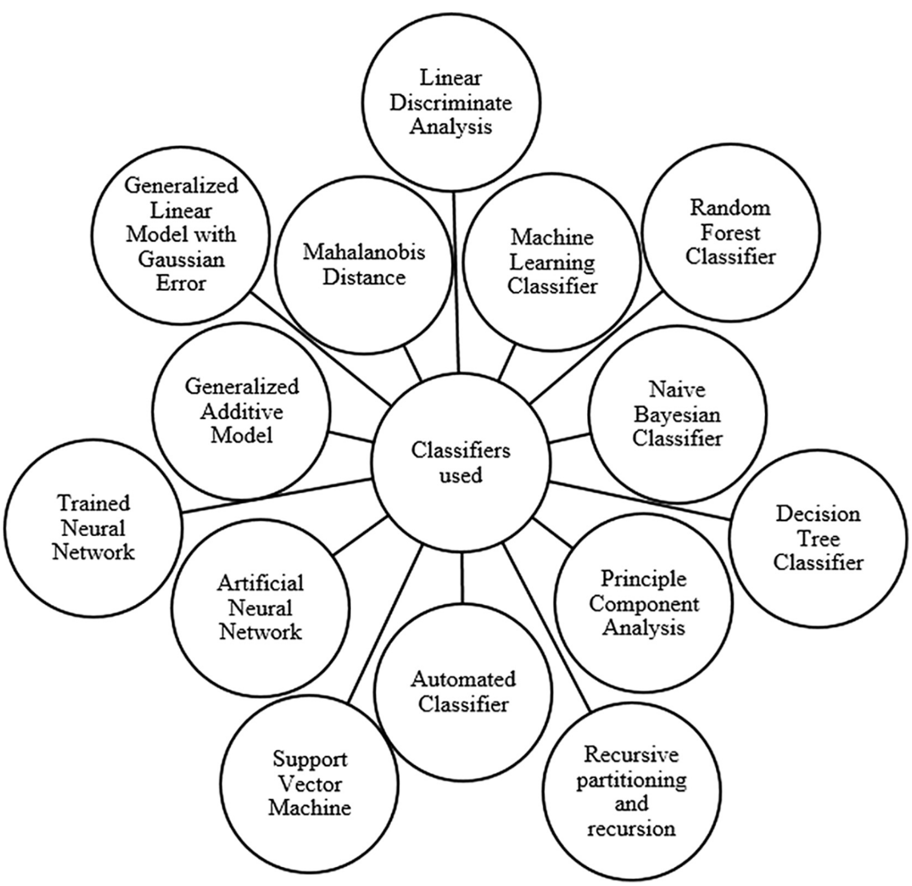

FIGURE 5 Classifiers used in glaucoma identification and detection (Masood, Sharif, Masood, Yasmin, & Raza, 2015; Masood, Sharif, Raza, et al., 2015)

analysis. The SVM and Gaussian mixture model (GMM) is used to employing the corresponding feature vectors and vessels in retinal images categorized as vessels and non-vessels. Xu and Luo (2010) counselled vessel segmentation associated with SVM for the combination of countless image processing methods. Normalized green channel background, for employing distinctive adaptive thresholding, the vast vessels are segmented, and the borders of optic disc are removed. For feature extraction, wavelets are used at several scales to process the initial image. Supervised learning is the way that the activities of the system are trained, instead of programmed. There is a larger encounter of machine learning classifier of input parameters for the diagnostic presentation. The diagnosis of glaucoma based on OCT can be enhanced through Machine learning classifiers (Bizios, Heijl, Hougaard, & Bengtsson, 2010). Keeping in mind the end goal to proficiently segregate amongst glaucomatous and solid eyes. Machine learning classifiers can be trained on SAP and OCT data. Enhancement in the diagnostic accuracy is achieved when the combination of SAP and OCT numbers as contrasted together with OCT data alone (Silva et al., 2013). LDA (Li & Yuan, 2005) uses parameters in linear combination to distinct glaucomatous and healthy eyes. The linear discriminate analysis gets image data, then forms a Gaussian allocation, and then alongside linear discrimination borders splits the data. An image analysis and association arrangement established on autonomous constituent image analysis or examination and k-nearest-neighbour association are used. Consequently, it achieves an association rate of 91% (Girard, Strouthidis, Ethier, & Mari, 2011). Global HRT parameters improves HRT parameter-based LDFs. Neural network explores the growing diagnostic accuracy of glaucoma tests (Xiangyu Chen et al. 2015). Zilly Buhmann, and Mahapatra (2017) on the basis of boosting applied convolution filter on convolution neural network (CNN). Marin, Aquino, Gegundez-Arias, and Bravo (2011) taken a shot at the division of retinal vessels and displayed a supervised strategy in light of neural system. Containing minute invariant-based elements and gray level this approach utilizes a 7-D feature vector. Table 5 shows the performances of some supervised learning methods.

5.2 | Unsupervised methods

The Unsupervised classification-based approaches are used to attempt to find retinal images inherent patterns whether the vessels belong to a particular pixel or not it does not depend on algorithm design. Tolias and Panas (1998) to track fundus vessel extraction in retinal angiogram images using linguistic descriptions by developing an algorithm using FCM clustering (Heckerman, Geiger, & Chickering, 1995). By using Naïve Bayesian method, the computational cost gets reduced (Clark, Zhang, & Yorio, 2010; Yager, 2006). Simo and de Ves (2001) and Sivak-Callcott, O'Day, Gass, and Tsai (2001) for the division of veins and supply routes utilize Bayesian investigation. The observed spatial intensities the stochastic model in light of a Gaussian clamor process is thought to be statically autonomous between the pixels. A clustering algorithm is combined with fractional supervision approach. Kande, Subbaiah, and Savithri (2010) propose a division

TABLE 5 Performances of some supervised learning methods

Methodology proposed by	Year	Classifier	No. of images	Specificity	Sensitivity	Accuracy
Nayak et al. (2009)	2009	ANN	61	100%	80%	–
U. Rajendra Acharya et al. (2015)	2015	SVM and naive Bayesian (NB)	510	89.75%	96.20%	93.10%
Dua et al. (Nath & Dandapat, 2012)	2012	SMO	60	–	–	93%
Kolar and Jan (Konstas et al., 2007)	2008	SVM	30	–	–	74%
Mookiah et al. (2012)	2012	SVM	60	93.33%	96.67%	95%
Osareh and Shadgar (2009)	2009	SVM, GMM	90	96.14	94.84%	95.24%
Xu and Luo (2010)	2010	SVM	90	–	0.7760	0.9328
Fink et al. (2008)	2008	KNN	120	–	–	91%
Nagarajan et al. (2002)	2002	ANN	399	95	94%	94%
Marin et al. (2011)	2011	Multilayer feed forward neural network	Drive, stare	0.7067 0.6944	0.9801 0.9819	0.9452 0.9526
Rüdiger Bock et al. (2010)	2010	SVM	575 Eigen images	88%	72%	78%
Muhammad et al. (2017)	2017	Random Forest	102	–	–	93.1%
Li et al. (2018)	2018	GON	8000	92.0%	95.6%	AUC 0.986

fuzzy method that utilizes the intensity information of a similar retinal image from red and green channels for the adjustment of nonuniform enlightenment. Coordinated sifting/Matched filtering is utilized to improve vein differentiation. At last, the spatially weighted fuzzy C-implies clustering is utilized at vascular tree structure distinguishing proof.

Figure 6 represent Optic disk Segmentation Process performed on color combination channel. First and fourth rows are normal images set. Second and third rows are images from the glaucomatous set. The Random Forest method (Lunetta, Hayward, Segal, & Van Eerdewegh, 2004; Strobl, Boulesteix, Zeileis, & Hothorn, 2007) as it comprises of many different decision trees is more robust to the problem of overfitting. As compared to decision tree method, the random forest's expectation accuracy is far more improved. Furthermore, OCT (Parvin, Alizadeh, & Minaei-Bidgoli, 2008) measurements are when distributed then there is considerable overlap between normal and glaucoma eyes, and hence limited diagnostic ability is achieved through a normative database when having a simple comparison of measurement parameters of OCT. Maroco et al. (2011) proposed estimates achieved from neuropsychological testing by using machine learning methods like Random Forests, Neural Networks, and SVM methods and methods derived from data mining using statistical classification increase accuracy, specificity, and also sensitivity (Strobl, Boulesteix, Kneib, Augustin, & Zeileis, 2008). Three traditional classifiers (Logistic Regression, Quadratic Discriminant Analysis, LDA) were looked at as far as general arrangement Press'Q, exactness, affectability, Area under the ROC bend, specificity to Seven nonparametric classifiers (Multilayer Perceptron, CHAID, Classification Trees, SVM, Neural Networks, CART, Radial Basis Function Neural Networks, QUEST and Random Forests). Statistical distributions of classification parameters were obtained compared using the Friedman's nonparametric test (Atto, Pastor, & Mercier, 2008). Decision tree classifier (Sugimoto et al., 2013) is a method used for recognizing pattern having if-then-else rules of a finite set and represented in a tree-like structure (Strobl, Malley, & Tutz, 2009; Sugimoto et al., 2013) The most common drawback that impacts the diagnostic accuracy of this method is the problem of "overfitting" (Narooie-Nejad et al., 2009). Indeed, in comparison with Random Forest method discriminating between pre-parametric and parametric glaucoma eyes, the decision tree method performed less accurately (Lisboa et al., 2013). A mix of phantom area intelligence tomography SD-OCT parameters is utilized to make a multivariable prescient model by utilizing EFA and Logistic Regression for glaucoma and outperformed classification rates, AUC, PILs, and AIC univariable models (Jiawei & Kamber, 2001). Takmaz and Can (2009) measured the glaucoma likelihood score GPS by contrasting affectability and specificity values for doing the separation amongst sound and glaucomatous eyes. HRT is measured through Moor field's regression analysis (MRA). It was considered that GPS has an advantage over MRA in the initial cases of glaucoma and it is also found that GPS might have better sensitivity but having worst specificity between glaucomatous and healthy eyes. Table 6 shows the performance measures of some unsupervised methods.

5.3 | Morphological processing methodologies

Segmentation is the procedure to reclaim the feature or ROI from an input image (Hameed, Sharif, Raza, Haider, & Iqbal, 2012; Shahzad, Sharif, Raza, & Hussain, 2008). The procedure is helpful as the main pre-processing period as well as request to recognize the meaningful data from healthy images. To attain the meaningful data, extra competent segmentation way is required. A little of the segmentation ways are edge detection, watershed algorithm and clustering (Ng, Ong, Foong, Goh, & Nowinski, 2006) Segmentation is the procedure to reclaim the feature or ROI from the input image. The procedure is helpful as the main pre-processing period as well as request to recognize the meaningful data from health images. To attain the meaningful data, extra competent segmentation way is required. A little of the segmentation ways are edge detection, wavelet feature (Singh, Dutta, ParthaSarathi, Uher, & Burget, 2016), watershed algorithm, and clustering.

Division of fundus color image for glaucoma recognition can also be gotten a handle out over the utilization of mathematical

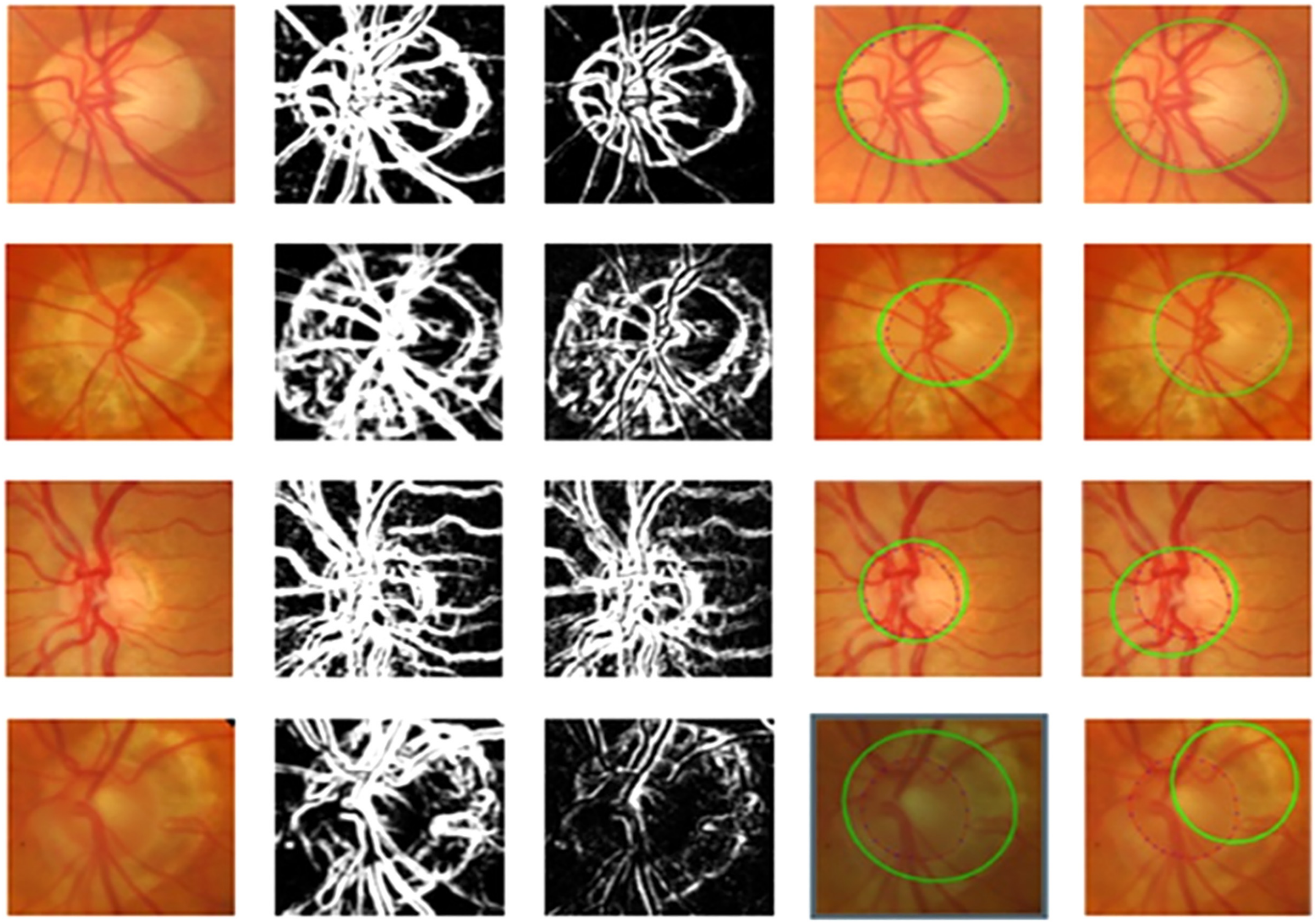

FIGURE 6 Optic disk segmentation process performed on color combination channel (Mohammed, Morris, & Thacker, 2014) [Color figure can be viewed at wileyonlinelibrary.com]

morphology. In progress to register the C/D proportion, creators have fragmented optic papilla/disk and ocular cup (Joshi, Sivaswamy, & Krishnadas, 2011). The optic papilla/disk detection is built upon format coordinating, contour perfect set up ways, Fuzzy convergence, geometric parametric perfect, and Hough transform. To discover the CDR values an ellipse fitting strategy is asked. Recursively bunching/clustering technique K-means (Figure 7e) is utilized so as to expel the optic papilla/disk and ocular cup range. The veins can be identified present in the zone of optic disk (OD) by utilizing distinctive entropy thresholding approach. By utilizing SVM, Bayes classifier and KNN for the relationship of fundus image and separating amongst ordinary and glaucomatous images by consolidating *C*/*D* proportion with the zone of veins in the inferior–superior side proportion than the territory of veins in the nasal-temporal side (ISNT) (see Figure 7 for details). Morphological strategies (Irum, Raza, & Sharif, 2012) can be used for the examination of the progression/movement of glaucoma. For the diagnosis of Glaucoma and other retinal diseases, (Naser Langroudi & Sadjedi, 2010) perform efficiently by considering optic disc features Blend of morphological techniques, edge identification, and feature/highlight extraction can be used for optic papilla/disk identification. Inadequate techniques for image upgrade contain histogram levelling/equalization, contrast extending and filtering (Burgansky-Eliash et al., 2005). There are various routes used for the upgrade reason. There are countless image enhancement methods (Shah, Khan, Shah, Raza, & Sharif, 2015) utilized for feature extraction and feature selection from the enumerated image to get the needed information. Most public utilized methods are histogram equalization, thresholding, green channel extraction, filtering, etc. Effects of Difference Enhancement and

TABLE 6 Performance measures of unsupervised methods

Methodology proposed by	Year	Classifier or methodology	No. of images/dataset	Specificity	Sensitivity	Accuracy
Salem et al. (2007)	2007	RACAL, KNN	Stare database	0.9750	0.8215	–
Kande et al. (2010)	2010	Fuzzy C-means clustering	Drive and stare database	–	–	ROC 0.9518, 0.9602
Joao Maroco et al. (2011)	2011	SVM, LDA, neural network	921	0.73	0.73	0.64
Mwanza et al. (2013)	2013	EFA and logistic	149	98.6%	96.0%	AIC 43.29
Takmaz et al. (2009)	2008	GPS, MRA	160	72.5%	93.8%	p = .317
Yoshida et al. (2014)	2014	Random forest, OCT	126	100–98.8%	80–90%	AROC 18.5 and 14.5
Abbas, Q. (2017)	2017	Unsupervised deep CNN	1200	98.01%	84.50%	99%

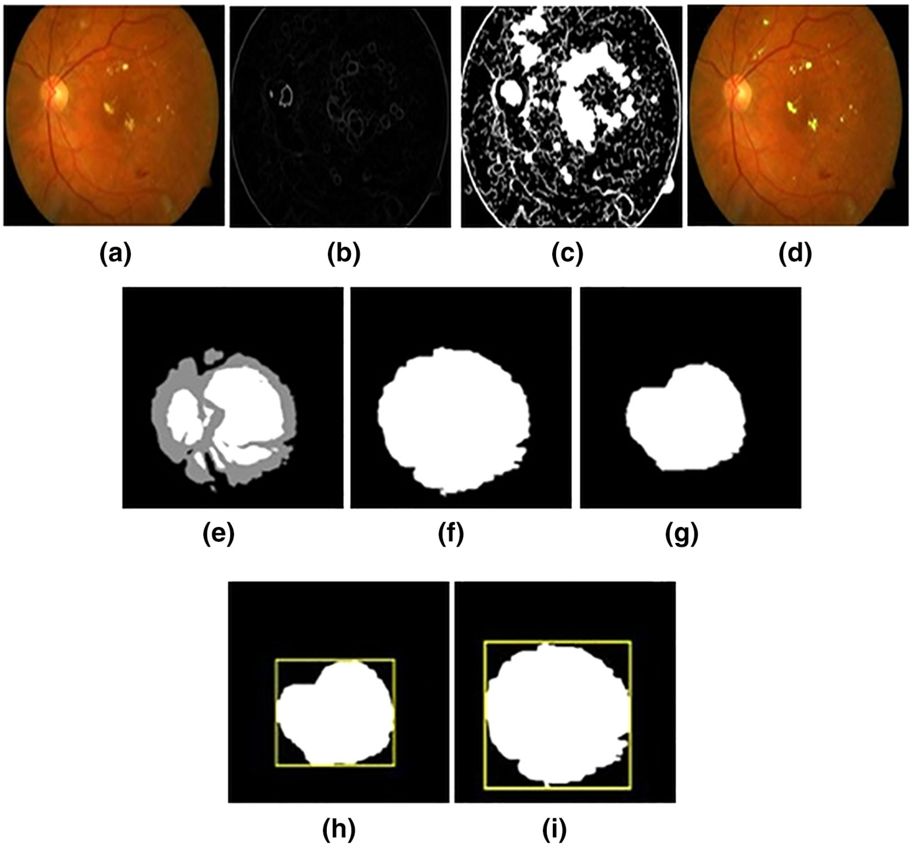

FIGURE 7 (a) Fundus image input, (b) gradient image dilation, (c) filtered and threshold image, (d) detection of exudates, (e) clustering using K-means, (f) OD detection, (g) detection of optic cup, (h) OD region, and (i) optic cup region (Pachiyappan, Das, Murthy, & Tatavarti, 2012) [Color figure can be viewed at wileyonlinelibrary.com]

Shadow Removal are given (Bock, Meier, Nyúl, Hornegger, & Michelson, 2010). MD is revealed effective in order to hold out the analogy measured from a recognized collection of sets. A database MS in a reference group including average deviations, mean and correlation construction in the reference collection (Miri et al., 2015). Table 7 shows Performance evaluations of some of morphological processing methodologies.

5.4 | Matched filtering methodologies

SVM detects essential parameters and overlooks less significant details. Ricci and Perfetti (2007) proposed pixel classification based on SVM and line operator's application as a feature vector. To accomplish unsupervised pixel classification, line detector calculates the average gray level that targets at different orientations along lines of fixed length then the threshold is achieved by applying the green channel. For building a feature vector by means of SVM among the gray level target pixels two orthogonal line detectors also get active. Both methods performance is evaluated that results in 0.9584, 0.9563 accuracies having ROC 0.9602, 0.9558 for STARE and DRIVE, correspondingly through ROC analysis of both datasets. Balasubramanian et al. (2010) estimated glaucomatous progression detection in humans. The Performance evaluations of some Matched Filtering Methodologies are given in Table 8.

TABLE 7 Performance measures of morphological processing methodologies

Methodology proposed by	Year	Classifier or methodology	No. of images/ dataset used	Specificity	Sensitivity	Accuracy
Naser Langroudi and Sadjedi (2010)	2010	OD segmentation and morphology	1863 images	81.4%	92.5%	–
Townsend et al. (2008)	2008	SVM, RPART, GLM, GAM	200	–	–	87.50%
Saleh et al. (2014)	2014	OD segmentation using FFT	DRIVE	91.27%	99.81%	98.68%
Zhang et al. (2010)	2010	GWA, SVM	SiMEs (691 images)	–	–	95.5%
Ahmed El-Rafei et al. (2013)	2013	SVM, GLCM, MD, ED	84 images	92.98%	96.30%	94.05%
Yousefi et al. (2014)	2014	GEM, linear regression	1095 images	87%	96%	–
Welfer et al. (2013)	2013	Mathematical morphology	DRIVE, DIARETDB1	99.81% 99.76%	83.54% 92.51%	97.75%
Fuente-Arriaga et al. (2014)	2014	Chessboard distance matrix, morphological features	67 images	91.66%	93.02%	91.34%

TABLE 8 Performance measures of matched filtering methodologies

Technique proposed by:	Year	No. of images	Methodology	Sensitivity	Specificity	Accuracy
Balasubramanian et al. (2010)	2010	12 primates (24 eyes)	Orthogonal Decomposition using SMO	–	–	AROC-0.94
Ricci and Perfetti (2007)	2007	Drive and stare database	SVM	–	–	0.9563, 0.9584
Belghith et al. (2014)	2014	246 images	SVM, SVDD, POD, TAC	86%	88%	–
Wong et al. (2008)	2008	ARGALIA 104 images	Level set based model	–	SD = 0.0597	96%
Salazar-Gonzalez et al. (2014)	2014	DIARETDB1, DRIVE, STARE	MRF	98.19% 87.50%	–	94.12%
Li and Chutatape (2003)	2003	65 images	ASM, PCA, model based approach	100%	71%	94%
Pal and Chatterjee (2017)	2017	20	Canny edge with Morphological operations	94.9%	98.74%	98.55%

5.5 | Multiscale approaches

Zhang, Liu, et al. (2010) encompassed optic cup detection through ellipse fitting and convex hull boundary flattering for level set segmentation by encouraging a merged way established on multimodalities. Almazroa Burman, Raahemifar, and Lakshminarayanan (2015) collected methods to enhance association accuracy for several classifiers using weighted combination methodologies. The integration of reliability compute enhances the classification presentation. A set of classifiers utilized to determine are (K-means clustering, Self-Organizing chart clustering, SVM, Fuzzy neural network, ANN, fuzzy c means clustering (Surendiran, Saravanan, & Elizabeth Catherine, 2016), K-means (Ayub, Ahmad, Muhammad, Aziz, & Ayub, 2016) classifier, Parzen classifier, Piecewise linear distance classifier, Piecewise quadratic distance classifier) are fixed that is, exceptionally for the request in hand, they are not optimized. To grasp reasonable association accuracy, different combination schemes are developed that is independent of the requested features. The extent of the classifier can be calculated through MK is Wk = 1/K. The bulk vote using this algorithm is more for subsequent probabilities if weights of classifiers are equal. By using Stratus OCT parameters as input, automated classifiers discriminate amongst normal and glaucomatous eyes. The multivariate data (MD) is measured through measurement space assembly, can forecast the severity of glaucoma. Later for glaucoma diagnosis PCA implementation result shows that the LDA and ANN are beaten by Mahalanobis space crafted by MD (Vingrys, 2000). Automated glaucoma diagnosis of digital fundus image arrangement employing HOS cumulants expelled from RT. The images are sorted into three classes: ordinary, mild, and moderate/serious glaucoma. For detection of glaucoma, the diagnostic performance is gasped out to ascertain using LDA and ANN to calculate whether LDA or ANN can differentiate amid vigorous eyes and glaucomatous eyes (Huang & Chen, 2005; Sharma, Sample, Zangwill, & Schuman, 2008). AROCs for the ANN and LDA methods were maximum achieved to be 0.970 for ANN and 0.950 for LDA while thinking Nerve Fibre Indicator 0.932. For the detection of glaucoma ANN, NFI, and LDF techniques clarified identical analytical manipulation implemented in a Taiwan Chinese population (Huang, Chen, Huang, & Tsai, 2010; Sakamoto et al., 2010). The learning skills of the neural network (Carmona, Rincón, García-Feijoó, & Martínez-de-la-Casa, 2008) are merged along with the estimated perceptive of fuzzy inference algorithms in the Adaptive Neuro-Fuzzy Inference System. For the detection of glaucoma, ANFIS-based learning models are developed for fundus images in order to categorize normal and typical images (Huang, Chen, & Huang, 2007) For achieving extremely good accuracy in optic cup detection, K-means clustering at every single pixel is utilized that enable quick clustering and focuses on the pallor data. As compared to the supervised method, it is easy and simplistic to apply unsupervised method. For precise detection of ocular papilla boundary, k means clustering,

TABLE 9 Performance measures of multi-scale approaches

Methodology proposed by	Year	Classifier	No. of images	Specificity	Sensitivity	Accuracy
Noronha et al. (2014)	2014	SVM, LDA, NB	272	100%	92%	92.65%
Yoshida et al. (2014)	2014	SVM, random forest	575	92.9%	96.0%	80%
Acharya et al. (2011)	2011	Naïve Bayesian, SVM, RF, SMO	60	–	–	91%
Huang and Chen (2005)	2005	LDA, MD, ANN, MD with PCA, LDA with PCA, ANN with PCA	89	100%	98.8%	–
Belghith et al. (2013)	2013	SVM, SVDD, MCMC, MRF, expectation–maximization algorithm	267	87%	91%	–
Huang et al. (2010)	2010	LDA, ANN	165	–	–	AROC-0.932
Kavitha (2012)	2012	ANFIS, SVM, neural network, K means clustering	550	97.6%	99.2%	98.7%
Kavitha (2012)	2012	BACKPROPAGATION, SVM, neural network	550	96.1%	97.7%	97.25%

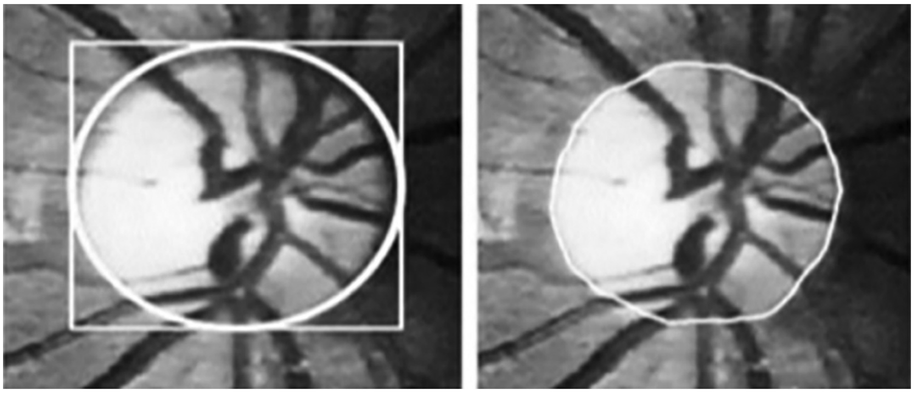

FIGURE 8 (a) the initial contour of OD detected ROI and (b) final contour of the OD obtained by GVF ACM (Chen et al. 2013)

and region growing methods provide an inspiring step. Table 9 shows the performance measures of some multi-scale approaches.

5.6 | Model-based segmentation approach

To accomplish a number of diseased images, Model established ways are used such as vessels association matched filtering, geometrical models and convergence of vasculature filter but they are computationally extremely expensive. As an early pace of localization process, the retinal vessels need to be segmented. Tobin et al. (2007) for localizing macula and optic nerve in fundus images (Tudor et al., 2014) utilized a geometrical model of the vasculature through optic nerve segmentation following facial feature determination. The retinal image describes average thickness, average orientation, and the density of the vasculature (Liang & Zeger, 1986). The Bayesian classifier is trained and applied to categorize a group of optic nerve pixels of the initial image to binary values of the optic nerve or non-optic nerve. Abdel Ghafar and Morris (2007) industrialized automated methods to produce quantitative descriptions of the retina to be utilized in diagnosis and treatment. Merely, the green channel was processed and OD boundary was noticed employing edge detector and circular Hough transform (Chen et al., 2013).

5.7 | Active contour model

In retinal fundus images, a statistics-based method is used in the optic disc for detecting the region of interest (ROI) (Figure 8a). From a set of rectangular regions having gray level pixels, ROI is chosen by applying this method by extracting statistical features like standard deviation and mean values in the candidate region. In the initial contour of the OD, ROI is treated as a highest inscribed circle and to exactly segment, the OD an active contour model (ACM) is used (Figure 8b). By combining ACM and statistics-based method, the OD segmentations impressive performance can be achieved (Xu, Chutatape, Sung, Zheng, & Kuan, 2007).

5.8 | Super pixel methods

A superpixel (SP) for glaucoma diagnosis is established discovering framework on retinal construction. This method utilizes constituent image automatically and localizes the optic cup for recognizing glaucoma in digital fundus photographs (Arnay et al. 2017; Xu et al., 2012). The main contributions provided by this method are three. Firstly, fundus images are used as it proposes super-pixel-based processing that leads to features extra illustrative, competent, and descriptive than others retained by pixel dependent methods, as compliant to substantial computational savings established on sliding windows. Besides, the classifier learning technique does not depend on prenamed preparing tests, yet rather the preparation illustrations are expelled from the examination image itself utilizing basic priors on near optic papilla (disk) and ocular cup positions. Thirdly, they introduced an affiliation refinement plot that uses both auxiliary (refinement) priors and neighbourhood (local) setting. Tried on a clinical dataset of ORIGA light involving 650 images, the proposed strategy accomplishes 0.081 distinct error CDR, a 26.7% non-overlap ratio (proportion) and a simple however widely used investigative measure (Tan, Xu, Goh, & Liu, 2015). In computer vision applications, superpixels (SP)—due to the upgraded introduction above pixel-based techniques—are ending up plainly progressively acknowledged. The fundus optic papilla (disk) images are divided into conservative, compact, and almost uniform SP utilizing SLIC algorithm (Dashtbozorg, Mendonça, & Campilho, 2015). Super-pixels do not divide the image of usual patches into the grid but have the vital property of maintaining distinctive boundaries (Cheng et al., 2013). The key parameter affecting the performance for super-pixel established ways is the number of SP that get affected in terms of both speed and accuracy. If SP are too huge then it leads to the ambiguity in labelled boundary by evolving super-pixel-based under-segmentation that requires more segmentation. After SP are excessively modest, the developing structures and features ascertained from the over-segmented ranges or area could come to be to some degree less unmistakable, making it additional intense to gather the right names. The most period expending part is feature (highlight) extraction for each and every SP, and got done with preparing period increments about straightly nearby the number of SP (Mittapalli & Kande, 2016). For 512, 256, and 2048 SP, the calculation seizes only 3.2, 1.7, and 20.2 s each image, separately. In Achanta et al. (2012) for glaucoma screening, the super-pixel based association is established amongst ocular cup and optic papilla segmentation. Glaucoma recognition or detection is assessed in patients employing multimodalities encompassing K-Means clustering, Gabor filter, and SLIC algorithm simple linear iterative clustering and colored fundus image to achieve exact edge allocation.

6 | DISCUSSION

There are countless areas of scrutiny in the prospect of glaucoma detection. According to the led scrutiny, there are disparate points that can be highlighted in this regard. The database utilization is the early traverse we can banter approximately. A large portion of the strategies for glaucoma location are surveyed on the publically evaluated databases. The quality of the techniques relies upon the database estimate. Enhanced fundus image is scarcely grasped out in the possibility of glaucoma detection however sensibly it is used as a preprocessing instrument. It is exceptionally hard to absolutely identify the optic papilla and the ocular cup since the nearness of different retinal sores, for example, hemorrhages, exudates, microaneurysms, veins, and low distinction of fundus images makes it intense for the exact recognition of optic plate limit. In image improvement ways, the greater part of the work is grasped out over the utilization of Green channel extraction, Thresholding, Histogram equalization and Filtering. In little cases, a blend of these ways is used to hold out this errand. Utilization of the green channel plane for the improvement system is by and large used in the input info forms/ processes. Feature extraction established approaches are extensively utilized for glaucoma recognition. These approaches are generally torn into supervised, unsupervised, multiscale, nonmodel based, model-based and matched filtering methods established features extraction. The bulk of the work is completed on the extraction of anatomical feature extraction. Glaucoma detection is scarcely grasped out by the way of textural established features. The amalgamation of these two kinds of structures can consequence in extra optimum resolutions for glaucoma recognition and identification. The sighting of glaucoma is primarily groundbreaking as it allows timely and convenient treatment to stop fundamental obvious vision misfortune. The glaucoma diagnosis can be proficient through measuring CDR. CDR is assessed by super-pixel affiliation strategy. The difficulty is that the ocular cup limits at the nasal side of the cup are oftentimes hard to discover because of the immediacy of vessels. This division involving multi-thresholding in that CDR is seen yet the misfortune is that the CDR estimation strategy is convoluted because of the vaguely depicted shading sense among the optic papilla and ocular cup. The OD fringes are not clear because of the habitations of vessels. Because of the sophistication of assets images, their lifted number of agents makes a flawless division troublesome. In future, we shall try to use super-pixel-based classification using different classifiers and try to get more accurate results for the automatic glaucoma detection.

7 | CONCLUSION

Glaucoma is one of the neurodegenerative maladies and is considered as one of the most widely recognized reasons for the visual impairment. Degeneration of nerves is an irreversible procedure, so the early finding of the illness is inescapable to maintain a strategic distance from lasting loss of vision. The article exhibits a diagram of the glaucoma malady, sorts, manifestations hazard, treatment, and image handling techniques proposed to analyze it. Diverse symptomatic methodologies have been checked on and broke down. Benefits and negative marks of every method have been explained by expressly introducing the situations where one plan is more fitting to use when contrasted with the other. Glaucoma is an illness for which clinical diagnosis is required. There does not exist any standard for measuring the progression of glaucoma. In our present structural techniques, as there is a lack of an ultimate computation, so it is hard to have certainty along the comparative specificities and sensitivities. Noticeably, improvements in structural and functional evaluation methods furnish additional goal precision and accuracy for the progression detection and diagnosis of the disease than the subjective and crude approaches of the past.

ORCID

Tanzila Saba https://orcid.org/0000-0003-3138-3801

REFERENCES

Abdel-Ghafar, R. A., & Morris, T. (2007). Progress towards automated detection and characterization of the optic disc in glaucoma and diabetic retinopathy. *Informatics for Health and Social Care*, *32*(1), 19–25.

Abdi, H., & Williams, L. J. (2010). Principal component analysis. *Wiley Interdisciplinary Reviews: Computational Statistics*, *2*(4), 433–459.

Achanta, R., Shaji, A., Smith, K., Lucchi, A., Fua, P., & Süsstrunk, S. (2012). SLIC superpixels compared to state-of-the-art superpixel methods. *IEEE Transactions on Pattern Analysis and Machine Intelligence*, *34*(11), 2274–2282.

Acharya, U. R., Dua, S., Du, X., Sree, S. V., & Chua, C. K. (2011). Automated diagnosis of glaucoma using texture and higher order spectra features. *IEEE Transactions on Information Technology in Biomedicine*, *15*(3), 449–455.

Acharya, U. R., Lim, C. M., Ng, E. Y. K., Chee, C., & Tamura, T. (2009). Computer-based detection of diabetes retinopathy stages using digital fundus images. *Proceedings of the Institution of Mechanical Engineers, Part H: Journal of Engineering in Medicine*, *223*(5), 545–553.

Acharya, U. R., Ng, E. Y. K., Eugene, L. W. J., Noronha, K. P., Min, L. C., Nayak, K. P., & Bhandary, S. V. (2015). Decision support system for the glaucoma using Gabor transformation. *Biomedical Signal Processing and Control*, *15*, 18–26. Available at:. http://linkinghub.elsevier.com/retrieve/pii/S1746809414001396

Akbar, S., Akram, M. U., Sharif, M., Tariq, A., & Yasin, U. U. (2017). Decision support system for detection of papilledema through fundus retinal images. *Journal of Medical Systems*, *41*(4), 66.

Akbar, S., Akram, M. U., Sharif, M., Tariq, A., & Yasin, U. U. (2018). Arteriovenous ratio and papilledema based hybrid decision support system for detection and grading of hypertensive retinopathy. *Computer Methods and Programs in Biomedicine*, *154*, 123–141.

Almazroa, A., Burman, R., Raahemifar, K., & Lakshminarayanan, V. (2015). Optic disc and optic cup segmentation methodologies for glaucoma image detection: A survey. *Journal of Ophthalmology*, *2015*, 1–28. Article ID 180972.

Amin, J., Sharif, M., & Yasmin, M. (2016). A review on recent developments for detection of diabetic retinopathy. *Scientifica*, *2016*, 1–20.

Amin, J., Sharif, M., Yasmin, M., Ali, H., & Fernandes, S. L. (2017). A method for the detection and classification of diabetic retinopathy using structural predictors of bright lesions. *Journal of Computational Science*, *19*, 153–164.

Anantrasirichai, N., Achim, A., Morgan, J. E., Erchova, I., & Nicholson, L. (2013). SVM-Based Texture Classification in Optical Coherence Tomography. *IEEE 10th International Symposium on Biomedical Imaging* (pp. 1320–1323). San Francisco, CA, USA.

Arnay, R., Fumero, F., & Sigut, J. (2017). Ant Colony optimization-based method for optic cup segmentation in retinal images. *Applied Soft Computing Journal*, *52*, 409–417.

Atto, A. M., Pastor, D., & Mercier, G. (2008). Detection threshold for non-parametric estimation. *Signal, Image and Video Processing*, *2*(3), 207–223.

Ayub, J., Ahmad, J., Muhammad, J., Aziz, L., & Ayub, S. (2016). Glaucoma detection through optic disc and cup segmentation using K-mean clustering. In *2016 International Conference on Computing, Electronic and Electrical Engineering, ICE Cube* (pp. 143–147), Quetta.

Balasubramanian, M., Bowd, C., Weinreb, R. N., Vizzeri, G., Alencar, L. M., Sample, P. A., … Zangwill, L. M. (2010). Clinical evaluation of the proper orthogonal decomposition framework for detecting glaucomatous changes in human subjects. *Investigative Ophthalmology and Visual Science*, *51*(1), 264–271.

Bauer, F., Pereverzev, S., & Rosasco, L. (2007). On regularization algorithms in learning theory. *Journal of Complexity*, *23*(1), 52–72.

Belghith, A., Balasubramanian, M., Bowd, C., Weinreb, R.N., & Zangwill, L. M. (2013). Glaucoma Progression Detection Using Variational Expectation Maximization Algorithm. *IEEE 10th International Symposium on Biomedical Imaging* (pp. 876–879). San Francisco, CA, USA.

Belghith, A., Balasubramanian, M., Bowd, C., Weinreb, R. N., & Zangwill, L. M. (2014). A unified framework for glaucoma progression detection using Heidelberg retina Tomograph images. *Computerized Medical Imaging and Graphics*, *38*(5), 411–420.

Betz, P., Camps, F., Collignon-Brach, J., Lavergne, G., & Weekers, R. (1982). Biometric study of the disc cup in open-angle glaucoma. *Graefes Archive for Clinical and Experimental Ophthalmology*, *218*(2), 70–74.

Bizios, D., Heijl, A., Hougaard, J. L., & Bengtsson, B. (2010). Machine learning classifiers for glaucoma diagnosis based on classification of retinal nerve fibre layer thickness parameters measured by stratus OCT. *Acta Ophthalmologica*, *88*(1), 44–52.

Bock, R., Jörg, M., Georg, M., László, N., & Joachim, H. (2007). *Classifying glaucoma with image-based features from fundus photographs* (pp. 355–364). Heidelberg: *Springer-Verlag*.

Bock, R., Meier, J., Nyúl, L. G., Hornegger, J., & Michelson, G. (2010). Glaucoma risk index: Automated glaucoma detection from color fundus images. *Medical Image Analysis*, *14*(3), 471–481.

Bokhari, F., Syedia, T., Sharif, M., Yasmin, M., & Fernandes, S. L. (2018). Fundus image segmentation and feature extraction for the detection of glaucoma: A new approach. *Current Medical Imaging Reviews*, *14*(1), 77–87.

Bokhari, S. T. F., Sharif, M., Yasmin, M., & Fernandes, S. L. (2017). Fundus image segmentation and feature extraction for the detection of glaucoma: A new approach. *Current Medical Imaging Reviews*, *13*, 1–10. Available at:. http://www.eurekaselect.com/node/151349/article

Bubella, R. M., Bubella, D. M., & Cillino, S. (2014). Type a behavior pattern: Is it a risk factor for open-angle chronic glaucoma? *Journal of Glaucoma*, *23*(4), 199–201.

Burgansky-Eliash, Z., Wollstein, G., Chu, T., Ramsey, J. D., Glymour, C., Noecker, R. J., … Schuman, J. S. (2005). Optical coherence tomography machine learning classifiers for glaucoma detection: A preliminary study. *Investigative Ophthalmology and Visual Science*, *46*(11), 4147–4152.

Carmona, E. J., Rincón, M., García-Feijoó, J., & Martínez-de-la-Casa, J. M. (2008). Identification of the optic nerve head with genetic algorithms. *Artificial Intelligence in Medicine*, *43*(3), 243–259.

Chen, H.-T., Wang, C.-M., Chan, Y.-K., Yang-Mao, S.-F., Chen, Y.-F., & Lin, S.-F. (2013). Statistics-based initial contour detection of optic disc on a retinal fundus image using active contour model. *Journal of Medical and Biological Engineering*, *33*(4), 388–393.

Chen, X., Xu, Y., Wong, D.W.K., Wong, T.Y., & Liu, J. (2015). Glaucoma detection based on deep convolutional neural network. C*onference proceedings : … Annual International Conference of the IEEE Engineering in Medicine and Biology Society (EMBC)*, *2015*, 715–718. Available at: http://ieeexplore.ieee.org/lpdocs/epic03/wrapper.htm?arnumber=7318462.

Cheng, J., Liu, J., Tao, D., Yin, F., Wong, D. W., Xu, Y., & Wong, T. Y. (2013). Superpixel classification based optic cup segmentation. In *International Conference on Medical Image Computing and Computer-Assisted Intervention* (pp. 421–428). Berlin, Heidelberg: Springer.

Cheng, J., Yin, F., Wong, D. W. K., Tao, D., & Liu, J. (2015). Sparse dissimilarity-constrained coding for glaucoma screening. *IEEE Transactions on Biomedical Engineering*, *62*(5), 1395–1403.

Choplin, N. T., & Traverso, C. E. (2014). *Atlas of glaucoma*. Boca Raton, London, New York: CRC Press.

Chrástek, R., Wolf, M., Donath, K., Niemann, H., Paulus, D., Hothorn, T., … Michelson, G. (2005). Automated segmentation of the optic nerve head for diagnosis of glaucoma. *Medical Image Analysis*, *9*(4), 297–314.

Clark, A. F., Zhang, X., & Yorio, T. (2010). Steroid-induced glaucoma. In *Ocular Disease: Mechanisms and Management* (pp. 146–152). China: Elsevier.

Dashtbozorg, B., Mendonça, A. M., & Campilho, A. (2015). Optic disc segmentation using the sliding band filter. *Computers in Biology and Medicine*, *56*, 1–12.

Dua, S., Acharya, U. R., Chowriappa, P., & Sree, S. V. (2012). Wavelet-based energy features for glaucomatous image classification. *IEEE Transactions on Information Technology in Biomedicine*, *16*(1), 80–87.

El-Rafei, A., Engelhorn, T., Wärntges, S., Dörfler, A., Hornegger, J., & Michelson, G. (2013). Glaucoma classification based on visual pathway analysis using diffusion tensor imaging. *Magnetic Resonance Imaging*, *31*(7), 1081–1091.

Fink, F., Worle, K., Gruber, P., Tome, A.M., Gorriz-Saez, J.M., Puntonet, C. G., & Lang, E.W. (2008). ICA analysis of retina images for glaucoma classification. *Conference proceedings: … Annual International Conference of the IEEE Engineering in Medicine and Biology Society*. *IEEE Engineering in Medicine and Biology Society*. *Conference*, 2008, 4664–4667. Available at: http://www.ncbi.nlm.nih.gov/pubmed/19163756.

Fraz, M. M., Remagnino, P., Hoppe, A., Uyyanonvara, B., Rudnicka, A. R., Owen, C. G., & Barman, S. A. (2012). Blood vessel segmentation methodologies in retinal images - a survey. *Computer Methods and Programs in Biomedicine*, *108*(1), 407–433.

Friedman, D. S., Wolfs, R. C., O'Colmain, B. J., Klein, B. E., Taylor, H. R., West, S., … Eye Diseases Prevalence Research Group. (2004). Prevalence of open-angle glaucoma among adults in the United States. *Archives of Ophthalmology (Chicago, Ill.: 1960)*, *122*(4), 532–538. http://www.ncbi.nlm.nih.gov/pubmed/15078671%5Cnhttp://www.pubmedcentral.nih.gov/articlerender.fcgi?artid=PMC2798086

Fuente-Arriaga, J. A., Felipe-Riverón, E. M., & Garduño-Calderón, E. (2014). Application of vascular bundle displacement in the optic disc for glaucoma detection using fundus images. *Computers in Biology and Medicine*, *47*(1), 27–35.

Giaconi, J. A., Law, S. K., & Nouri-Mahdavi, K. (Eds.). (2016). *Pearls of glaucoma management* (2nd ed.). Berlin, Heidelberg: Springer.

Girard, M. J. A., Strouthidis, N. G., Ethier, C. R., & Mari, J. M. (2011). Shadow removal and contrast enhancement in optical coherence tomography images of the human optic nerve head. *Investigative Ophthalmology and Visual Science*, *52*(10), 7738–7748.

Gordon, M. O., Beiser, J. A., Brandt, J. D., Heuer, D. K., Higginbotham, E. J., Johnson, C. A., … Kass, M. A. (2002). The ocular hypertension treatment study: Baseline factors that predict the onset of primary open-angle glaucoma. *Archives of Ophthalmology*, *120*(6), 714–720. http://www.ncbi.nlm.nih.gov/pubmed/12049575

Greenfield, D. S., Liebmann, J. M., Ritch, R., Krupin, T., & Low-Pressure Glaucoma Study Group. (2007). Visual field and intraocular pressure asymmetry in the low-pressure glaucoma treatment study. *Ophthalmology*, *114*(3), 460–465.

Hameed, M., Sharif, M., Raza, M., Haider, S. W., & Iqbal, M. (2012). Framework for the comparison of classifiers for medical image segmentation with transform and moment based features. *Research Journal of Recent Sciences*, *2277*, 2502.

He, L., Yang, H., Gardiner, S. K., Williams, G., Hardin, C., Strouthidis, N. G., … Burgoyne, C. F. (2013). Longitudinal detection of optic nerve head changes by spectral domain optical coherence tomography in early experimental glaucoma. *Investigative Ophthalmology and Visual Science*, *55*(1), 574–586.

Heckerman, D., Geiger, D., & Chickering, D. M. (1995). Learning Bayesian networks: The combination of knowledge and statistical data. *Machine Learning*, *20*(3), 197–243.

Heryadi, Y., Fanany, M.I., & Arymurthy, A.M. (2013). Stochastic regular grammar-based learning for basic dance motion recognition. In *2013 International Conference on Advanced Computer Science and Information Systems*, ICACSIS 2013, 419–424.

Hoover, A. (2000). Locating blood vessels in retinal images by piecewise threshold probing of a matched filter response. *IEEE Transactions on Medical Imaging*, *19*(3), 203–210.

Huang, M. L., & Chen, H. Y. (2005). Development and comparison of automated classifiers for glaucoma diagnosis using stratus optical coherence tomography. *Investigative Ophthalmology and Visual Science*, *46*(11), 4121–4129.

Huang, M. L., Chen, H.-Y., & Huang, J.-J. (2007). Glaucoma detection using adaptive neuro-fuzzy inference system. *Expert Systems with Applications*, *32*(2), 458–468. Available at:. http://linkinghub.elsevier.com/retrieve/pii/S0957417405003568

Huang, M. L., Chen, H. Y., Huang, W. C., & Tsai, Y. Y. (2010). Linear discriminant analysis and artificial neural network for glaucoma diagnosis using scanning laser polarimetry-variable cornea compensation measurements in Taiwan Chinese population. *Graefe's Archive for Clinical and Experimental Ophthalmology*, *248*(3), 435–441.

Irum, I., Raza, M., & Sharif, M. (2012). Morphological techniques for medical images: A review. *Research Journal of Applied Sciences*, *4*, 2948–2962.

Irum, I., Shahid, M. A., Sharif, M., & Raza, M. (2015). A review of image Denoising methods. *Journal of Engineering Science & Technology Review*, *8*(5), 41–48.

Irum, I., Sharif, M., Raza, M., & Mohsin, S. (2015). A nonlinear hybrid filter for Salt & Pepper Noise Removal from color images. *Journal of Applied Research and Technology*, *13*(1), 79–85.

Irum, I., Sharif, M., Raza, M., & Yasmin, M. (2015). Salt and pepper noise removal filter for 8-bit images based on local and global occurrences of Grey levels as selection indicator. *Nepal Journal of Science and Technology*, *15*(2), 123–132.

Irum, I., Sharif, M., Yasmin, M., Raza, M., & Azam, F. (2015). A noise adaptive approach to impulse noise detection and reduction. *Nepal Journal of Science and Technology*, *15*(1), 67–76.

Jiawei, H., & Kamber, M. (2001). *Data mining: concepts and techniques.* Retrieved from http://scholar.google.com/scholar?hl=en&btnG=Search&q=intitle:Data+mining+concepts+and+techniques#1%5Cnhttp://scholar.google.com/scholar?hl=en&btnG=Search&q=intitle:Data+mining:+concepts+and+techniques%231%5Cnhttp://scholar.google.com/scholar?hl=en&btnG=S.

Jonas, J. B., Aung, T., Bourne, R. R., Bron, A. M., Ritch, R., & Panda-Jonas, S. (2017). Glaucoma. *The Lancet*, *390*, 2183–2193.

Joshi, G. D., Sivaswamy, J., & Krishnadas, S. R. (2011). Optic disk and cup segmentation from monocular color retinal images for glaucoma assessment. *IEEE Transactions on Medical Imaging*, *30*(6), 1192–1205.

Kande, G. B., Subbaiah, P. V., & Savithri, T. S. (2010). Unsupervised fuzzy based vessel segmentation in pathological digital fundus images. *Journal of Medical Systems*, *34*(5), 849–858.

Kauppi, T., Kalesnykiene, V., Kamarainen, J.-K., Lensu, L., Sorri, I., Raninen, A., … Pietila, J. (2007). the DIARETDB1 diabetic retinopathy database and evaluation protocol. In *Procedings of the British Machine Vision Conference* (pp. 15.1–15.10). Warwick, UK. Available at: http://www.bmva.org/bmvc/2007/papers/paper-60.html.

Khaimi, M. A. (2015). Canaloplasty: A minimally invasive and maximally effective glaucoma treatment. *Journal of Ophthalmology*, *2015*, 485065.

Khan, M. W., Sharif, M., Yasmin, M., & Fernandes, S. L. (2016). A new approach of cup to disk ratio based glaucoma detection using fundus images. *Journal of Integrated Design and Process Science*, *20*(1), 77–94.

Khan, M. W., Sharif, M., Yasmin, M., & Saba, T. (2017). CDR based glaucoma detection using fundus images: A review. *International Journal of Applied Pattern Recognition*, *4*(3), 261–306.

Kim, M. J., Kim, M. J., Kim, H. S., Jeoung, J. W., & Park, K. H. (2014). Risk factors for open-angle glaucoma with normal baseline intraocular pressure in a young population: The Korea National Health and nutrition examination survey. *Clinical & Experimental Ophthalmology*, *42*(9), 825–832.

Konstas, A. G. P., Kozobolis, V. P., Katsimpris, I. E., Boboridis, K., Koukoula, S., Jenkins, J. N., & Stewart, W. C. (2007). Efficacy and safety of Latanoprost versus Travoprost in exfoliative glaucoma patients. *Ophthalmology*, *114*(4), 653–657.

Köse, C., & Ikibaş, C. (2011). A personal identification system using retinal vasculature in retinal fundus images. *Expert Systems with Applications*, *38*(11), 13670–13681.

Kourkoutas, D., Karanasiou, I. S., Tsekouras, G. J., Moshos, M., Iliakis, E., & Georgopoulos, G. (2012). Glaucoma risk assessment using a non-linear multivariable regression method. *Computer Methods and Programs in Biomedicine*, *108*(3), 1149–1159.

Li, H., & Chutatape, O. (2003). A model-based approach for automated feature extraction in fundus images. Proceedings Ninth IEEE International Conference on Computer Vision (pp. 394–399). Nice, France. Available at: http://ieeexplore.ieee.org/xpls/abs_all.jsp?arnumber=1238371.

Li, H., Lim, J. H., Liu, J., Mitchell, P., Tan, A. G., Wang, J. J., & Wong, T. Y. (2010). A computer-aided diagnosis system of nuclear cataract. *IEEE Transactions on Biomedical Engineering*, *57*(7), 1690–1698.

Li, H., Lim, J.H., Liu, J., Wing, D., Wong, K., & Wong, T.Y. (2010). Feature analysis in slit-lamp image for nuclear cataract diagnosis. In *Proceedings - 2010 3rd International Conference on Biomedical Engineering and Informatics, BMEI 2010* (pp. 253–256), Yantai, China.

Li, M., & Yuan, B. (2005). 2D-LDA: A statistical linear discriminant analysis for image matrix. *Pattern Recognition Letters*, *26*(5), 527–532.

Li, Z., He, Y., Keel, S., Meng, W., Chang, R. T., & He, M. (2018). Efficacy of a deep learning system for detecting glaucomatous optic neuropathy based on color fundus photographs. *Ophthalmology*, *125*(8), 1199–1206.

Liang, K. Y., & Zeger, S. L. (1986). Longitudinal data analysis using generalized linear models. *Biometrika*, *73*(1), 13–22.

Lisboa, R., Paranhos, A., Jr., Weinreb, R. N., Zangwill, L. M., Leite, M. T., & Medeiros, F. A. (2013). Comparison of different spectral domain OCT scanning protocols for diagnosing preperimetric glaucoma. *Investigative Ophthalmology and Visual Science*, *54*(5), 3417–3425.

Lunetta, K. L., Hayward, L. B., Segal, J., & Van Eerdewegh, P. (2004). Screening large-scale association study data: Exploiting interactions using random forests. *BMC Genetics*, *5*(1), 32.

Manners, T., Salmon, J. F., Barron, A., Willies, C., & Murray, A. D. (2001). Trabeculectomy with mitomycin C in the treatment of post-traumatic angle recession glaucoma. *The British Journal of Ophthalmology*, *85*(2), 159–163.

Marin, D., Aquino, A., Gegundez-Arias, M. E., & Bravo, J. M. (2011). A new supervised method for blood vessel segmentation in retinal images by using gray-level and moment invariants-based features. *IEEE Transactions on Medical Imaging*, *30*(1), 146–158.

Maroco, J., Silva, D., Rodrigues, A., Guerreiro, M., Santana, I., & de Mendonça, A. (2011). Data mining methods in the prediction of dementia: A real-data comparison of the accuracy, sensitivity and specificity of linear discriminant analysis, logistic regression, neural networks, support vector machines, classification trees and random forests. *BMC Research Notes*, *4*(1), 299. Available at:. http://www.biomedcentral.com/1756-0500/4/299

Masood, S., Sharif, M., Masood, A., Yasmin, M., & Raza, M. (2015). A survey on medical image segmentation. *Current Medical Imaging Reviews*, *11*(1), 3–14.

Masood, S., Sharif, M., Raza, M., Yasmin, M., Iqbal, M., & Younus Javed, M. (2015). Glaucoma disease: A survey. *Current Medical Imaging Reviews*, *11*(4), 272–283.

Mermoud, A., Schnyder, C. C., Sickenberg, M., Chiou, A. G., Hédiguer, S. E., & Faggioni, R. (1999). Comparison of deep sclerectomy with collagen implant and trabeculectomy in open-angle glaucoma. *Journal of Cataract and Refractive Surgery*, *25*(3), 323–331. http://www.ncbi.nlm.nih.gov/pubmed/10079436

Michelson, G., Wärntges, S., Hornegger, J., & Lausen, B. (2008). The papilla as screening parameter for early diagnosis of glaucoma. *Deutsches Arzteblatt International*, *105*(34–35), 583–589.

Miglior, S., Guareschi, M., Albe', E., Gomarasca, S., Vavassori, M., & Orzalesi, N. (2003). Detection of glaucomatous visual field changes using the Moorfields regression analysis of the Heidelberg retina tomograph. *American Journal of Ophthalmology*, *136*(1), 26–33.

Miguel-Jiménez, J. M., Boquete, L., Ortega, S., Rodríguez-Ascariz, J. M., & Blanco, R. (2010). Glaucoma detection by wavelet-based analysis of the global flash multifocal electroretinogram. *Medical Engineering and Physics*, *32*(6), 617–622.

Miri, M. S., Abramoff, M. D., Lee, K., Niemeijer, M., Wang, J. K., Kwon, Y. H., & Garvin, M. K. (2015). Multimodal segmentation of optic disc and cup from SD-OCT and color fundus photographs using a machine-learning graph-based approach. *IEEE Transactions on Medical Imaging*, *34*(9), 1854–1866.

Mittapalli, P. S., & Kande, G. B. (2016). Segmentation of optic disk and optic cup from digital fundus images for the assessment of glaucoma. *Biomedical Signal Processing and Control*, *24*, 34–46.

Mohammed, S., Morris, T., & Thacker, N. (2014). Optic disk segmentation using texture. In: Proceedings of the 9th International Conference on Computer Vision Theory and Application (Vol. 1, pp. 293–300). Lisbon, Portuga.

Mookiah, M. R. K., Rajendra Acharya, U., Lim, C. M., Petznick, A., & Suri, J. S. (2012). Data mining technique for automated diagnosis of glaucoma using higher order spectra and wavelet energy features. *Knowledge-Based Systems*, *33*, 73–82.

Muhammad, H., Fuchs, T. J., De Cuir, N., De Moraes, C. G., Blumberg, D. M., Liebmann, J. M., … Hood, D. C. (2017). Hybrid deep learning on single wide-field optical coherence tomography scans accurately classifies glaucoma suspects. *Journal of Glaucoma*, *26*(12), 1086–1094.

Mwanza, J.-C., Warren, J. L., & Budenz, D. L. (2013). Combining spectral domain optical coherence tomography structural parameters for the diagnosis of glaucoma with early visual field loss. *Investigative Ophthalmology & Visual Science*, *54*(13), 8393–8400. http://www.ncbi.nlm.nih.gov/pubmed/24282232

Narooie-Nejad, M., Paylakhi, S. H., Shojaee, S., Fazlali, Z., Rezaei Kanavi, M., Nilforushan, N., … Paisán-Ruiz, C. (2009). Loss of function mutations in the gene encoding latent transforming growth factor beta binding protein 2, LTBP2, cause primary congenital glaucoma. *Human Molecular Genetics*, *18*(20), 3969–3977.

Naser Langroudi, M., & Sadjedi, H. (2010). A new method for automatic detection and diagnosis of retinopathy diseases in colour fundus images based on Morphology. 2010 International Conference on Bioinformatics and Biomedical Technology (pp. 134–138). Chengdu, China. Available at: http://ieeexplore.ieee.org/lpdocs/epic03/wrapper.htm?arnumber=5478995.

Nath, M. K., & Dandapat, S. (2012). Techniques of glaucoma detection from color fundus images: A review. *International Journal of Image, Graphics and Signal Processing*, *4*(9), 44–51.

Nayak, J., Acharya, U. R., Bhat, P. S., Shetty, N., & Lim, T. C. (2009). Automated diagnosis of glaucoma using digital fundus images. *Journal of Medical Systems*, *33*(5), 337–346.

Newman-Casey, P. A., Talwar, N., Nan, B., Musch, D. C., & Stein, J. D. (2011). The relationship between components of metabolic syndrome and open-angle glaucoma. *Ophthalmology*, *118*(7), 1318–1326.

Ng, D. S. C., Ching, R. H. Y., & Chan, C. W. N. (2015). Angle-recession glaucoma: Long-term clinical outcomes over a 10-year period in traumatic microhyphema. *International Ophthalmology*, *35*(1), 107–113.

Ng, H.P., Ong, S.H., Foong, K.W.C., Goh, P.S., & Nowinski, W.L. (2006). Medical Image Segmentation Using K-Means Clustering and Improved Watershed Algorithm. *2006 I.E. Southwest Symposium on Image Analysis and Interpretation* (pp. 61–65). Denver, CO, USA. Available at: http://ieeexplore.ieee.org/lpdocs/epic03/wrapper.htm?arnumber=1633722.

Noronha, K. P., Acharya, U. R., Nayak, K. P., Martis, R. J., & Bhandary, S. V. (2014). Automated classification of glaucoma stages using higher order cumulant features. *Biomedical Signal Processing and Control*, *10*(1), 174–183.

Ny´ul, L.G. (2009). Retinal image analysis for automated glaucoma risk evaluation. In *Proceedings of SPIE - The International Society for Optical Engineering*, Yichang, China.

Osareh, A., & Shadgar, B. (2009). Automatic blood vessel segmentation in color images of retina. *Iranian Journal of Science and Technology Transaction B Engineering*. *33*, 191–206. Available at:. http://www.sid.ir/En/VEWSSID/J_pdf/8542009B205.pdf

Pachiyappan, A., Das, U. N., Murthy, T. V., & Tatavarti, R. (2012). Automated diagnosis of diabetic retinopathy and glaucoma using fundus and OCT images. *Lipids in Health and Disease*, *11*(1), 73.

Pal, S., & Chatterjee, S. (2017). Mathematical morphology aided optic disk segmentation from retinal images. 2017 3rd International Conference on Condition Assessment Techniques in Electrical Systems (CATCON) (pp. 380–385). IEEE. Rupnagar, India.

Parvin, H., Alizadeh, H., & Minaei-Bidgoli, B. (2008). A new approach to improve the vote-based classifier selection. In *Proceedings - 4th International Conference on Networked Computing and Advanced Information Management, NCM 2008* (pp. 91–95). Gyeongju, South Korea.

Qureshi, I., Sharif, M., Yasmin, M., Raza, M., & Javed, Y. M. (2016). Computer aided systems for diabetic retinopathy detection using digital fundus images: A survey. *Current Medical Imaging Reviews*, *12*(4), 234–241.

Ricci, E., & Perfetti, R. (2007). Retinal blood vessel segmentation using line operators and support vector classification. *IEEE Transactions on Medical Imaging*, *26*(10), 1357–1365.

Roodhooft, J. M. (2002). Leading causes of blindness worldwide. *Bulletin de la Société Belge d'Ophtalmologie*, *283*, 19–25.

Rosenfeld, C., Price, M. O., Lai, X., Witzmann, F. A., & Price, F. W., Jr. (2015). Distinctive and pervasive alterations in aqueous humor protein composition following different types of glaucoma surgery. *Molecular Vision*, *21*, 911.

Sakamoto, A., Hangai, M., Nukada, M., Nakanishi, H., Mori, S., Kotera, Y., … Yoshimura, N. (2010). Three-dimensional imaging of the macular retinal nerve fiber layer in glaucoma with spectral-domain optical coherence tomography. *Investigative Ophthalmology & Visual Science*, *51*(10), 5062–5070.

Salazar-Gonzalez, A., Kaba, D., Li, Y., & Liu, X. (2014). Segmentation of blood vessels and optic disc in retinal images. *IEEE Journal of Biomedical and Health Informatics*, *18*(6), 1874–1886. Available at:. http://ieeexplore.ieee.org/lpdocs/epic03/wrapper.htm?arnumber=6725621

Saleh, M.D., Salih, N.D., Eswaran, C., & Abdullah, J. (2014). Automated segmentation of optic disc in fundus images. In: 2014 I.E. 10th International Colloquium on signal processing & its applications (CSPA) (pp. 145–150). Piscataway: IEEE.

Salem, S. A., Salem, N. M., & Nandi, A. K. (2007). Segmentation of retinal blood vessels using a novel clustering algorithm (RACAL) with a partial supervision strategy. *Medical and Biological Engineering and Computing*, *45*(3), 261–273.

Shabbir, B., Sharif, M., Nisar, W., Yasmin, M., & Fernandes, S. L. (2016). Automatic cotton wool spots extraction in retinal images using texture segmentation and gabor wavelet. *Journal of Integrated Design and Process Science*, *20*(1), 65–76.

Shah, G. A., Khan, A., Shah, A. A., Raza, M., & Sharif, M. (2015). A review on image contrast enhancement techniques using histogram equalization. *Science International*, *27*(2), 1297–1302.

Shahzad, A., Sharif, M., Raza, M., & Hussain, K. (2008). Enhanced watershed image processing segmentation. *Journal of Information & Communication Technology*, *2*(1), 01–09.

Sharif, M., Irum, I., Yasmin, M., & Raza, M. (2017). Salt & Pepper Noise Removal from Digital Color Images Based on Mathematical Morphology and Fuzzy Decision. *Nepal Journal of Science and Technology*, *18*(1), 1–7.

Sharma, P., Sample, P. A., Zangwill, L. M., & Schuman, J. S. (2008). Diagnostic tools for glaucoma detection and management. *Survey of Ophthalmology*, *53*(6), S17–S32.

Silva, F. R., Vidotti, V. G., Cremasco, F., Dias, M., Gomi, E. S., & Costa, V. P. (2013). Sensitivity and specificity of machine learning classifiers for glaucoma diagnosis using spectral domain oct and standard automated perimetry. *Arquivos Brasileiros de Oftalmologia*, *76*(3), 170–174.

Simó, A., & de Ves, E. (2001). Segmentation of macular fluorescein angiographies. A statistical approach. *Pattern Recognition*, *34*(4), 795–809. Available at:. http://www.sciencedirect.com/science/article/B6V14-42407P3-5/2/4ab40e4e5f1f571a369a2c82223f6342

Singh, A., Dutta, M. K., ParthaSarathi, M., Uher, V., & Burget, R. (2016). Image processing based automatic diagnosis of glaucoma using wavelet features of segmented optic disc from fundus image. *Computer Methods and Programs in Biomedicine*, *124*, 108–120.

Sivak-Callcott, J. A., O'Day, D. M., Gass, J. D., & Tsai, J. C. (2001). Evidence-based recommendations for the diagnosis and treatment of neovascular glaucoma. *Ophthalmology*, *108*(10), 1767–1776, 1800. Available at:. http://eutils.ncbi.nlm.nih.gov/entrez/eutils/elink.fcgi?dbfrom=pubmed&id=11581047&retmode=ref&cmd=prlinks%5Cnpapers2://publication/uuid/BA1C5BFD-0662-478C-B02F-F8535F027AA4

Sng, C. C., Foo, L. L., Cheng, C. Y., Allen, J. C., He, M., Krishnaswamy, G., … Aung, T. (2012). Determinants of anterior chamber depth: The Singapore Chinese eye study. *Ophthalmology*, *119*(6), 1143–1150.

Sommer, A., Tielsch, J. M., Katz, J., Quigley, H. A., Gottsch, J. D., Javitt, J., & Singh, K. (1991). Relationship between intraocular pressure and primary open angle glaucoma among white and black Americans: The Baltimore eye survey. *Archives of Ophthalmology*, *109*(8), 1090–1095.

Staal, J. J., Abramoff, M. D., Niemeijer, M., Viergever, M. A., & van Ginneken, B. (2004). DRIVE: Digital retinal images for vessel extraction. *IEEE Transactions on Medical Imaging*, *23*, 501–509. Available at:. http://www.isi.uu.nl/Research/Databases/DRIVE/

Staal, J. J., Abràmoff, M. D., Niemeijer, M., Viergever, M. A., & van Ginneken, B. (2005). Ridge based vessel segmentation in color images of the retina. *IEEE Transactions on Medical Imaging*, *23*(4), 501–509. Available at:. http://www.isi.uu.nl/Research/Publications/publicationview.php?id=855

Station, W. (2007). Predictive factors for open-angle glaucoma among patients with ocular hypertension in the European glaucoma prevention study. *Ophthalmology*, *114*(1), 3–9.

Strobl, C., Boulesteix, A. L., Kneib, T., Augustin, T., & Zeileis, A. (2008). Conditional variable importance for random forests. *BMC Bioinformatics*, *9*(1), 307. http://bmcbioinformatics.biomedcentral.com/articles/10.1186/1471-2105-9-307

Strobl, C., Boulesteix, A. L., Zeileis, A., & Hothorn, T. (2007). Bias in random forest variable importance measures: Illustrations, sources and a solution. *BMC Bioinformatics*, *8*, 25. http://www.ncbi.nlm.nih.gov/pubmed/17254353

Strobl, C., Malley, J., & Tutz, G. (2009). An introduction to recursive partitioning: Rationale, application, and characteristics of classification and regression trees, bagging, and random forests. *Psychological Methods*, *14*(4), 323–348. Available at:. http://doi.apa.org/getdoi.cfm?doi=10.1037/a0016973

Sugimoto, K., Murata, H., Hirasawa, H., Aihara, M., Mayama, C., & Asaoka, R. (2013). Cross-sectional study: Does combining optical coherence tomography measurements using the "random Forest" decision tree classifier improve the prediction of the presence of perimetric deterioration in glaucoma suspects? *BMJ Open*, *3*(10), e003114. Available at:. http://www.pubmedcentral.nih.gov/articlerender.fcgi?artid=3796272&tool=pmcentrez&rendertype=abstract

Sung, K. R., Kim, J. S., Wollstein, G., Folio, L., Kook, M. S., & Schuman, J. S. (2011). Imaging of the retinal nerve fibre layer with spectral domain optical coherence tomography for glaucoma diagnosis. *The British Journal of Ophthalmology*, *95*(7), 909–914. http://www.ncbi.nlm.nih.gov/pubmed/21030413

Surendiran, J., Saravanan, S. V., & Elizabeth Catherine, F. (2016). Glaucoma detection using fuzzy C-mean (FCM). *International Journal of Pharmacy and Technology*, *8*(3), 16149–16163.

Takmaz, T., & Can, I. (2009). Comparison of glaucoma probability score and Moorfields regression analysis to discriminate glaucomatous and healthy eyes. *European Journal of Ophthalmology*, *19*(2), 207–213.

Tan, N. M., Xu, Y., Goh, W. B., & Liu, J. (2015). Robust multi-scale superpixel classification for optic cup localization. *Computerized Medical Imaging and Graphics*, *40*, 182–193.

Tolias, Y. A., & Panas, S. M. (1998). A fuzzy vessel tracking algorithm for retinal images based on fuzzy clustering. *IEEE Transactions on Medical Imaging*, *17*(2), 263–273. Available at:. http://www.scopus.com/inward/record.url?eid=2-s2.0-0032034235&partnerID=40&md5=2983ba7daa85a19aee72982cdcca4705

Tobin, K. W., Chaum, E., Govindasamy, V. P., & Karnowski, T. P. (2007). Detection of anatomic structures in human retinal imagery. *IEEE transactions on medical imaging*, *26*(12), 1729–1739.

Toshev, A. P., Lamparter, J., Pfeiffer, N., & Hoffmann, E. M. (2017). Bruch's membrane opening-minimum rim width assessment with spectral-domain optical coherence tomography performs better than confocal scanning laser ophthalmoscopy in discriminating early glaucoma patients from control subjects. *Journal of Glaucoma*, *26*(1), 27–33. Available at:. http://content.wkhealth.com/linkback/openurl?sid=WKPTLP:landingpage&an=00061198-201701000-00005

Townsend, K. A., Wollstein, G., Danks, D., Sung, K. R., Ishikawa, H., Kagemann, L., … Schuman, J. S. (2008). Heidelberg retina Tomograph 3 machine learning classifiers for glaucoma detection. *The British Journal of Ophthalmology*, *92*(6), 814–818.

Tudor, D., Kajić, V., Rey, S., Erchova, I., Považay, B., Hofer, B., … Morgan, J. E. (2014). Non-invasive detection of early retinal neuronal degeneration by ultrahigh resolution optical coherence tomography. *PLoS One*, *9*(4), e93916.

Vingrys, A. J. (2000). The many faces of glaucomatous optic neuropathy. *Clinical & Experimental Optometry*, *83*(3), 145–160. http://www.ncbi.nlm.nih.gov/pubmed/12472447

Wang, X., Khan, R., & Coleman, A. (2015). Device-modified trabeculectomy for glaucoma. *The Cochrane Database of Systematic Reviews*, *12*(12), CD010472.

Welfer, D., Scharcanski, J., & Marinho, D. R. (2013). A morphologic two-stage approach for automated optic disk detection in color eye fundus images. *Pattern Recognition Letters*, *34*(5), 476–485.

Wong, D.K., Liu, J., Lim, J.H., Jia, X., Yin, F., Li, H., & Wong, T.Y. (2008). Level-set based automatic cup-to-disc ratio determination using retinal fundus images in Argali. *Conference proceedings: … Annual International Conference of the IEEE Engineering in Medicine and Biology Society. IEEE Engineering in Medicine and Biology Society. Annual Conference*, *2008*(2), 2266–2269.

Xu, J., Chutatape, O., Sung, E., Zheng, C., & Kuan, P. C. T. (2007). Optic disk feature extraction via modified deformable model technique for glaucoma analysis. *Pattern Recognition*, *40*(7), 2063–2076.

Xu, L., & Luo, S. (2010). A novel method for blood vessel detection from retinal images. *BioMedical Engineering OnLine*, *9*(1), 14. Available at:. http://biomedical-engineering-online.biomedcentral.com/articles/10.1186/1475-925X-9-14

Xu, Y., Liu, J., Lin, S., Xu, D., Cheung, C.Y., Aung, T., & Wong, T.Y. (2012). Efficient optic cup detection from intra-image learning with retinal structure priors. *Medical image computing and computer-assisted intervention : MICCAI … International Conference on Medical Image Computing and Computer-Assisted Intervention*, *15*(Pt 1), 58–65. Available at: http://www.ncbi.nlm.nih.gov/pubmed/23285535.

Yager, R. R. (2006). An extension of the naive Bayesian classifier. *Information Sciences*, *176*(5), 577–588.

Yasmin, M., Sharif, M., & Mohsin, S. (2013). Neural networks in medical imaging applications: A survey. *World Applied Sciences Journal*, *22*(1), 85–96.

Yin, F., Liu, J., Wong, D.W.K., Tan, N.M., Lee, B.H., Cheng, J., … Gao, X. (2013). ACHIKO-I retinal fundus image database and its evaluation on cup-to-disc ratio measurement. In *Proceedings of the 2013 I.E. 8th Conference on Industrial Electronics and Applications* (pp. 224–227). *ICIEA*.

Yoshida, T., Iwase, A., Hirasawa, H., Murata, H., Mayama, C., Araie, M., & Asaoka, R. (2014). Discriminating between glaucoma and normal eyes using optical coherence tomography and the "random forests" classifier. *PLoS One*, *9*(8), e106117.

Yousefi, S., Goldbaum, M. H., Balasubramanian, M., Medeiros, F. A., Zangwill, L. M., Liebmann, J. M., … Bowd, C. (2014). Learning from data: Recognizing glaucomatous defect patterns and detecting progression from visual field measurements. *IEEE Transactions on Biomedical Engineering*, *61*(7), 2112–2124.

Zafar, R., Sharif, M., & Yasmin, M. (2018). A survey on the prevalence of cataract and its accompanying risk factors. *Current Medical Imaging Reviews*, *14*(2), 251–262.

Zhang, Z., Liu, J., Yin, F., Lee, B.-H., Wong, D.W.K., & Sung, K.R. (2013). ACHIKO-K: Database of fundus images from glaucoma patients. In *Proceedings of the 2013 I.E. 8th Conference on Industrial Electronics and Applications* (pp. 228–231). *ICIEA*..

Zhang, Z., Liu, J., Kwoh, C.K., Sim, X., Tay, W.T., Tan, Y., … Wong, T.Y. (2010). Learning in glaucoma genetic risk assessment. Conference proceedings : … Annual International Conference of the IEEE Engineering in Medicine and Biology Society. Annual conference, 2010, 6182–6185.

Zilly, J., Buhmann, J. M., & Mahapatra, D. (2017). Glaucoma detection using entropy sampling and ensemble learning for automatic optic cup and disc segmentation. *Computerized Medical Imaging and Graphics*, *55*, 28–41.

How to cite this article: Saba T, Bokhari STF, Sharif M, Yasmin M, Raza M. Fundus image classification methods for the detection of glaucoma: A review. *Microsc Res Tech*. 2018; 81:1105–1121. https://doi.org/10.1002/jemt.23094